

UNCLASSIFIED

AD 286 925

*Reproduced
by the*

**ARMED SERVICES TECHNICAL INFORMATION AGENCY
ARLINGTON HALL STATION
ARLINGTON 12, VIRGINIA**



UNCLASSIFIED

NOTICE: When government or other drawings, specifications or other data are used for any purpose other than in connection with a definitely related government procurement operation, the U. S. Government thereby incurs no responsibility, nor any obligation whatsoever; and the fact that the Government may have formulated, furnished, or in any way supplied the said drawings, specifications, or other data is not to be regarded by implication or otherwise as in any manner licensing the holder or any other person or corporation, or conveying any rights or permission to manufacture, use or sell any patented invention that may in any way be related thereto.

63-1-3

10

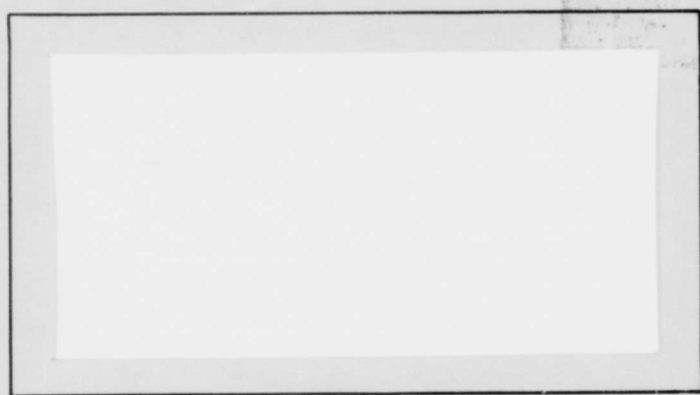
286925
286925

AIR FORCE INSTITUTE OF TECHNOLOGY



AIR UNIVERSITY
UNITED STATES AIR FORCE

AD No. _____
ASTIA FILE COPY



286 925

SCHOOL OF ENGINEERING

WRIGHT-PATTERSON AIR FORCE BASE, OHIO

ASTIA
RECEIVED
OCT 30 1962
TISIA

AF-WP-O-MAY 62 3,500

\$7.60

**AN INVESTIGATION OF THE USE OF RADIATION FROM
RADIOISOTOPES TO MEASURE DENSITY ALTITUDE**

THESIS

GA/Phys/62-13

Alexander Kratz Rupp

Capt USAF

**AN INVESTIGATION OF THE USE OF RADIATION FROM
RADIOISOTOPES TO MEASURE DENSITY ALTITUDE**

THESIS

**Presented to the Faculty of the School of Engineering of
the Air Force Institute of Technology
Air University
in Partial Fulfillment of the
Requirements for the Degree of
Master of Science**

By

Alexander Kratz Rupp, B.S.

Capt

USAF

Graduate Astronautical Engineering

August 1962

Preface

As a pilot I have been long aware that the altitude limitation of the barometric altimeters is in the neighborhood of 100,000 feet, but I was surprised to learn that as yet no workable aircraft altimeter has been designed to operate at higher altitudes. When Mr. Paul Polishuk of the Flight Control Laboratories at Wright-Patterson Air Force Base suggested an experiment to investigate the use of a radioisotope as an altimeter, I became much intrigued with this device as a subject for independent study.

I must say that without the guidance of my advisor, Dr. George John, I would have been out of my depth. As for Mr. Polishuk and his laboratory, they were available for much needed help at any time, which I gratefully acknowledge. Mr. Laugle and Mr. Miller, foremen at the Environmental and Propulsion Altitude Chambers, respectively, were invaluable in their physical assistance as were Mr. Wolf of the school shops and Mr. Miskimen, Mr. Hendricks, Mr. Elsworth, and Airman First Class Nixon of the AFIT Physics Laboratory.

Alexander K. Rupp

Contents

	Page
Preface	ii
List of Figures	v
List of Graphs	vi
Abstract	vii
I. Introduction	1
II. Types of Radioisotope Altimeters	3
Alpha Sources	3
Absorption	3
Residual Range	4
Fluorescent Screen	6
Gamma, X-Ray, and Bremsstrahlung Sources	7
Beta Sources	8
Attenuation	8
Backscatter	9
Small-Angle Scatter	11
Criteria and Selection of Small-Angle Scatter	13
III. Theoretical Background for Small-Angle Scatter	15
Rutherford Scattering	15
Theoretical Prediction of Scattering Intensity	18
IV. Experimental Design of Small-Angle-Scatter Altimeter	21
Preliminary Design	21
Isotope	21
Source	21
Source Collimator	23
Detectors	23
First Experimental Design	25
Isotope	25
Source	25
Source Collimator	27
Detector Collimator	27
Detector	29
Electronics	31

Contents

	Page
V. Testing	32
Initial Testing	32
Atmosphere Testing	32
Environmental Chamber Tests	32
Final Design and Propulsion Chamber Tests	42
VI. Summary of Important Results and Conclusions	52
Bibliography	54
Appendix A: Air and Spacecraft Operating at 100,000 Foot Altitude and Above	56
Appendix B: Distinction Between True, Absolute, Pressure, and Density Altitudes with Significance of Density Altitude for Aerodynamic Flight	58
Appendix C: Calculation of Theoretical Count Rate as a Function of Density Altitude Using Bullard and Massey Graphical Solution	59
Appendix D: Altitude-Pressure Table Used in Environmental Chamber Tests	64
Appendix E: Altitude-Pressure Table Used in Propulsion Chamber Tests	65
Appendix F: Random Error and Altimeter Lag Error Analysis of Experimental Small-Angle- Beta-Scatter-Density Altimeter	66
Vita	70

List of Figures

Figure		Page
1	Graph Showing Determination of Alpha Range in Geiger-Nuttal Experiment	3
2	Bragg Ionization Curve for Polonium Alpha Source	4
3	Schopper's Method of Density Determination Using Alpha Residual Ionization	5
4	Schumacher's Fluorescent Screen Method of Altitude Measurement with Alpha Particles	6
5	Schematic Diagram of Beta Beam Attenuator	8
6	Strontium ⁹⁰ Response Curve in Air at a Fixed Distance From Detector as a Function of Density	9
7	Beta Backscatter Altimeter	10
8	Schumacher's Proposal for Small-Angle Scatter Altimeter	12
9	Trajectory of Rutherford Electron Scatter	16
10	Bullard and Massey Graphical Solution of Rutherford Scattering Equation	19
10a	Theoretical Determination of Count Rates as a Function of Density Altitude	20
11	Penetration Ability of Beta Radiation	22
12	Source and Source Collimator	26
13	Detector Collimator	28
14	Detector	30
15	Chamber Wall Backscatter	39
16	Experiment to Measure Effect of Chamber Wall Backscatter	40
17	Vacuum Box for Pre-Amplifier	45
18	Assembly for Final Small-Angle Beta Scatter Experiment	48
19	Penumbra Radiation	50
20	Experiment to Eliminate Penumbra Radiation	51

List of Graphs

Graph	Page
I Atmospheric Test	33
II First Environmental Chamber Test	37
III Second Environmental Chamber Test	39a
IV Third Environmental Chamber Test	41
IVa Error Envelope Resulting from Statistical Variations and Altimeter Lag	43
V Propulsion Chamber Tests	49

Abstract

The purpose of this investigation is to review all known methods that obtain density altimetry from the radiation of radioisotopes and to report upon the results of testing one of the methods, small-angle-beta scatter, in an altitude chamber. The nature of the problem requires that the range of density altitude to be measured is from 100,000 feet to 300,000 feet, and within this range the small-angle-beta-scatter altimeter proves to offer a satisfactory theoretical solution. Final experimental construction of such an altimeter employs a 2/10 curie strontium ⁹⁰ yttrium ⁹⁰ source, the beta radiation of which is collimated by an aluminum tube shielded by lead and iron. After small angle scatter in air occurs, the beta radiation is re-collimated and detected by an anthracene scintillating crystal and associated electronic equipment. The count rate of the apparatus is a decreasing function with increasing altitude, and it is this observation that makes the small-angle-beta-scatter gage useful as an altimeter. Testing showed that final results in an altitude chamber provide readable data from 100,000 feet to 210,000 feet. In the conclusion it is noted that the small-angle-beta-scatter-density altimeter is especially suitable for mounting in hypersonic aircraft because it samples ambient air, requires no compressibility corrections, and can be located in fuselage areas of relatively low temperature that require no special protection.

AN INVESTIGATION OF THE USE OF RADIATION FROM
RADIOISOTOPES TO MEASURE DENSITY ALTITUDE

I. Introduction

The purpose of this thesis is twofold: to discuss possible methods of obtaining altimetry above 100,000 feet and to report on the theoretical operation, experimental design, and results obtained from altitude chamber tests of one of the promising methods, small-angle-scatter of beta rays in air. The scope of the study is restricted to devices whose operation is based upon the interaction of radiation from selected radioisotopes with the atmosphere.

A brief survey of the operational altitudes of several weapons systems, some in existence, some soon to be in existence, can be found in Appendix A. The F-104, X-15, Mercury, Gemini, Dynasoar, and Apollo all exceed 100,000 feet in operation. In comparison, the limit of the present day barometric altimeter is 100,000 feet (Ref 6:4-3). The nature of the problem, then, is to fill the altimeter gap between 100,000 feet and 300,000 feet, the latter figure being the von Karman Line (Ref 20:28) which marks the end of the lift capability from aircraft control surfaces.

The solution to this problem was successful to the extent that an experimental radioisotope density-altimeter did operate in an altitude chamber in the range of 100,000 feet to 210,000 feet. In addition, based on this study further improvements are suggested that may increase the measurable altitude range to above 300,000 feet.

The format of the text is as follows: First, in Chapter II a survey of all known methods of using radioisotopes for altimeters is made, and their advantages and disadvantages are listed. Then one of the methods, small-angle-beta scatter, is selected for experimental study, and the reasons for this choice are enumerated. In Chapter III the theoretical background for small-angle-beta scatter is investigated, and a means for graphically obtaining a theoretical beta cross section for scatter as a function of density altitude is reproduced and explained.

In the next two chapters, IV and V, considerations that determined the preliminary design of the experimental apparatus are discussed; the alterations of the preliminary design that resulted from tests are explained; and the final design specifications are set forth. Finally, following Chapter VI which is devoted to results, information is given in Appendix A concerning the altitude capabilities of all weapons systems that operate within the range of this study. In Appendix B is presented the difference between true altitude, absolute altitude, pressure altitude, and density altitude, with special emphasis upon the significance of density altitude for aerodynamic flight. Appendix C is the calculation of the theoretical count rate of a beta-scatter altimeter as a function of density altitude. The pressure altitude tables used in the altitude chambers are found in Appendixes D and E, while Appendix F gives a theoretical study of statistical error and altimeter lag error of the final experimental design.

II. Types of Radioisotope Altimeters

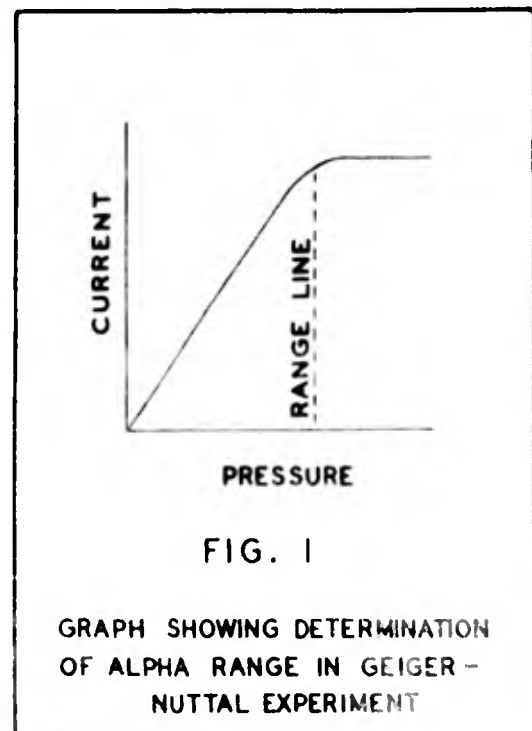
Alpha Sources

Absorption. An adaptation of the experimental method of Geiger and Nuttall for measuring the range of alpha particles in air is suggested by Wright and Hakevessel (Ref 20:41) for acquiring altitude information.

If an alpha source is placed on the end of a metallic rod in the center of a glass bulb which is silvered on the inside and a high voltage is applied to the bulb and rod, a current will flow which is proportional to the amount of ionization caused by the alpha particles passing through the air of the bulb. As the air pressure increases, so does the current, until all the alpha particles are absorbed. At this point further ionization of the air cannot take place, and an increase of air pressure is without effect. At the point where the current rise ceases, which is labeled "Range Line" in

Fig. 1, the alpha particles just reach the wall of the bulb, and the bulb radius becomes the range at that pressure. This was the method of Geiger and Nuttall (Ref 19:247).

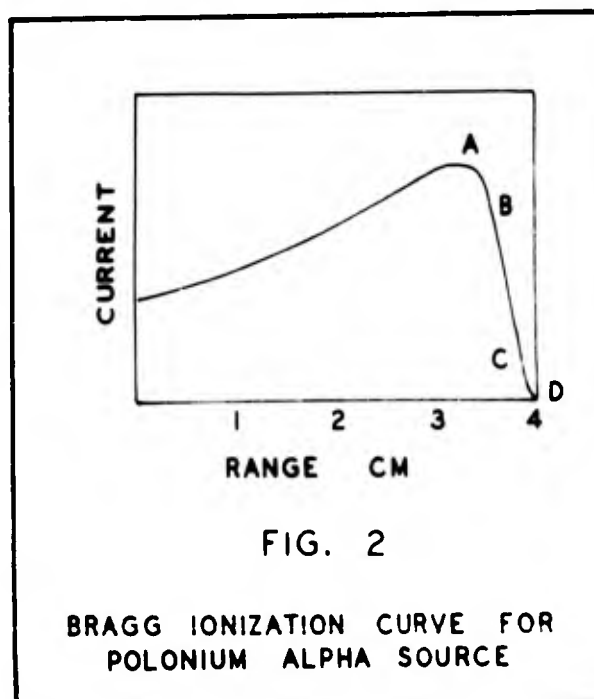
Since the range in a gas is inversely proportional to the pressure,



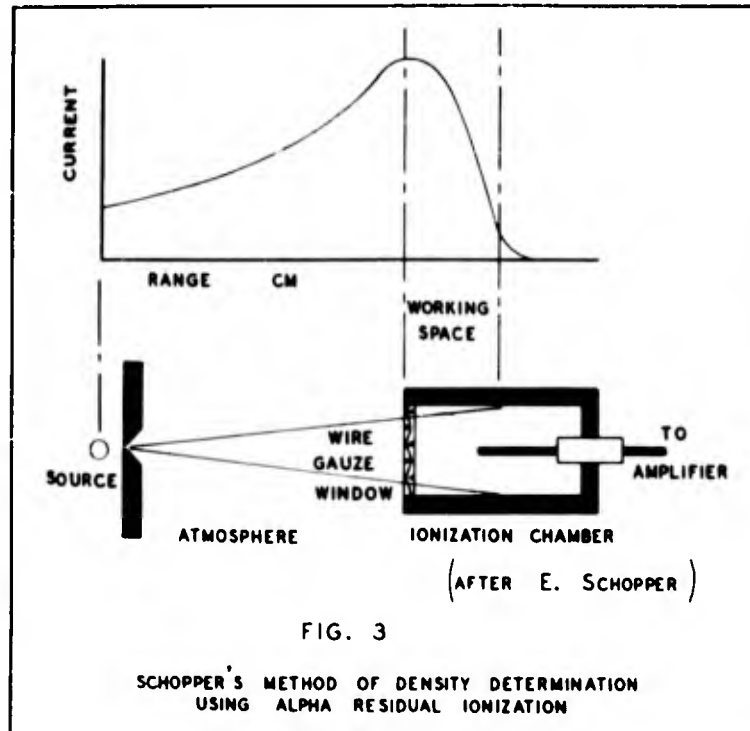
Wright and Hakewessel have suggested varying the source-to-detector geometry in order to seek the "Range Line" and arrive at an indication of air density directly (Ref 20:41). The monoenergetic characteristic of the alpha particles affords mathematical convenience and allows easy discrimination against background radiation, but the necessity of a movable platform aboard an aircraft presents very serious structural and technical disadvantages.

Residual Range. The Bragg Ionization Curve is shown in Fig. 2 for a Polonium alpha source, $E = 5.3$ Mev, to picture how the ionization produced by the alpha rays increases at first gradually, then more markedly until it reaches a peak, after which it decreases rapidly to zero. It should be noted that the line BC is nearly linear and can be fixed with a great degree of empirical certainty, while the pronounced tail of the curve

is not nearly so certain, because of the difficulty of experimentally determining points on an asymptotic curve (Ref 11a:69). A device which measures the residual ionization after the peak of the Bragg Curve has been designed by E. Schopper (Ref 16:2) and is shown in Fig. 3 on the following page.



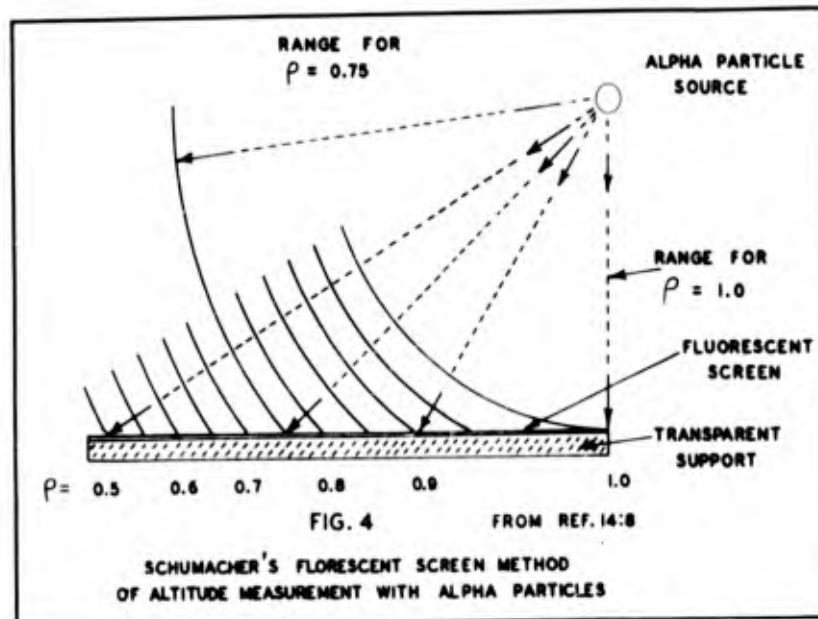
The Bragg Curve is drawn again to relate the position of the ionization chamber to the residual (decreasing) ionization curve. The principle of



operation is that a very slight increase in atmospheric density shortens the range of the alpha particles, shifts the Bragg Curve to the left, and reduces the ionization current recorded. Precise measurements are possible because of the very rapid change in current with a small change in range. The Schopper method uses a wire window over the entrance to the ionization chamber to prevent ions within, momentarily uncounted, from being sucked out by the Bernoulli Action of the flowing gas stream outside (Ref 16:2), although what effect upon measured ionization will be produced by supersonic and hypersonic gas flows is not yet known. If the residual-range altimeter is to be used in the non-linear

regions AB or CD, calibration of the instrument is required. Of more serious concern is the disadvantage that the density range covered is small unless a variable geometry is introduced, and this in turn brings about serious aircraft structure and technical problems.

Fluorescent Screen. In the fluorescent screen method of density altitude measurement suggested by Schumacher (Ref 14:1-5), a point alpha source is placed opposite the screen as pictured in Fig. 4. The perpendicular distance between the screen and the source is chosen so that when the density of the intervening gas is equal to one (which can be any reference density desired), the alpha particle range will just equal



the perpendicular distance, and only a spot of the screen will phosphor. As the density of the gases decreases, the spherical surface which represents the range of the alpha particle beam becomes larger. This transforms the fluorescent point into an ever increasing circle, since

whenever the alpha particles strike the screen it will fluoresce, while beyond the range of the alpha particles the screen remains dark. The radius of the illuminated area is seen to be a measure of the range of the alpha particles and, consequently, of the atmospheric gas density. Detection devices for the luminous area could be photomultiplier tubes or phototransistors. This design has the advantage of no moving parts and simplicity, but it does present the problem of requiring an enormously large screen if changes in density of up to four orders of magnitude are required. Accuracy of the screen method would be affected at small angles of incidence (long ranges) by the slight but discernible multi-energies of the alpha particles (Ref 11a:47).

Gamma, X-Ray, and Bremsstrahlung Sources

The absorption process of gamma, x-ray, and bremsstrahlung radiation is so negligible in rarefied air that it may be neglected (Ref 20:69), and the usefulness of this process for an altimeter is doubtful. Work has been done using soft x-ray absorption to measure densities of air streams in supersonic wind tunnels, but the adaptation of such highly specialized wind tunnel equipment to an aircraft altimeter is not considered feasible for numerous reasons¹ (Ref 20:12 and Ref 4:92).

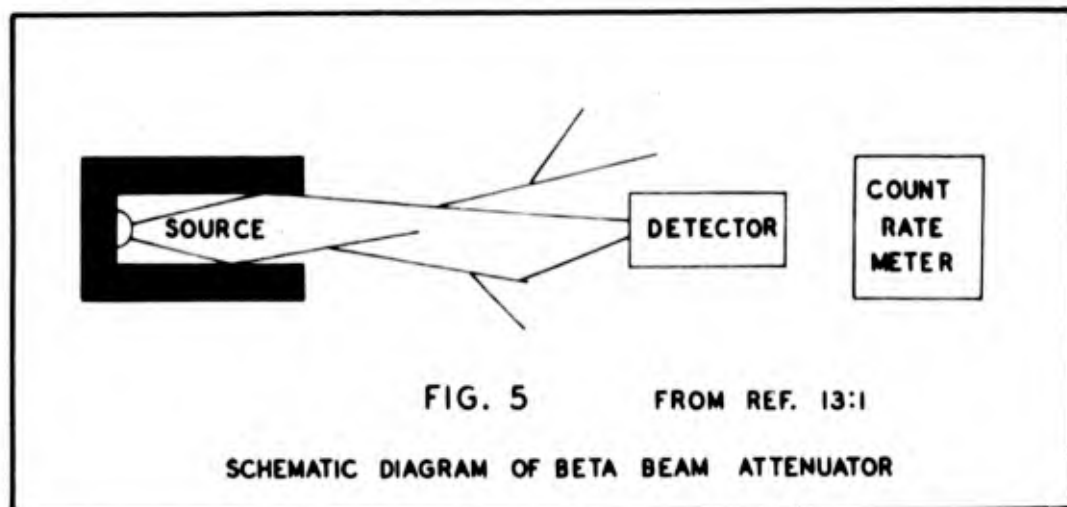
Scattering of photons in air above 10 Kev depends only upon the free electron density, which even for dissociated atoms is proportional

¹The major objection to the Knight and Venable Method (Ref 7) is the requirement for the addition of one of the rare gases, such as krypton, to the airstream flow, which is impossible in an aircraft altimeter. The objection to the NACA procedure (Ref 4) is that the time response of the device to pressure changes varies from 5 minutes to 30 seconds, which is clearly unsuitable for use as an altimeter.

to the air density; hence, the possibility of using gamma, x-ray, or bremsstrahlung radiation for measuring density altitudes in the 100,000 feet to 300,000 feet region does exist. It has been suggested that the 6 Kev x-rays from Fe^{55} and the 1 Kev bremsstrahlung from a tritium target are suitable sources of radiation (Ref 20:70). As yet, no known photon-scattering-density altimeter has been constructed.

Data Sources

Attenuation. The electron beam probe for measuring gas densities has these decided advantages: it responds nearly exactly to density; it is not affected by the gas velocity or turbulence, and not even by smoke, dust, or steam; it works at every temperature; and it has been successfully used in the entire pressure range from 10^3 torr (one torr equals one mm Hg) to 50×10^{-3} torr² (Ref 13:110 and Ref 5:273). Beam attenuation from a gage constructed as in Fig. 5 relies on the fact that



² 50×10^{-3} torr represents an altitude of 230,000 feet.

there is an exponential reduction in the counting rate with increasing density. A typical response curve, plotting count rate vs. density ρ_0 , is shown in Fig. 6. An interplay between the exponential attenuation and the statistical fluctuations of the radiation exists, however, which limits the useful

accuracy of the gage to density measurements over a range of one order of magnitude (for example, from 1000 torr to 100 torr). Since the range required for a gage operating within the 100,000 feet to 300,000 feet region of the atmosphere is from 10 torr to 10^{-3} torr, it can be understood that

this method has very definite drawbacks for use as an altimeter.

Backscatter. Two Boeing Aircraft engineers have constructed an experimental beta backscatter altimeter that has worked well from 10,000 feet to 66,000 feet (Ref 1:124). The principal advantage of this altimeter is the compact geometrical arrangement of the components, which fit into a probe 30 inches long as shown in Fig. 7 on the following page.

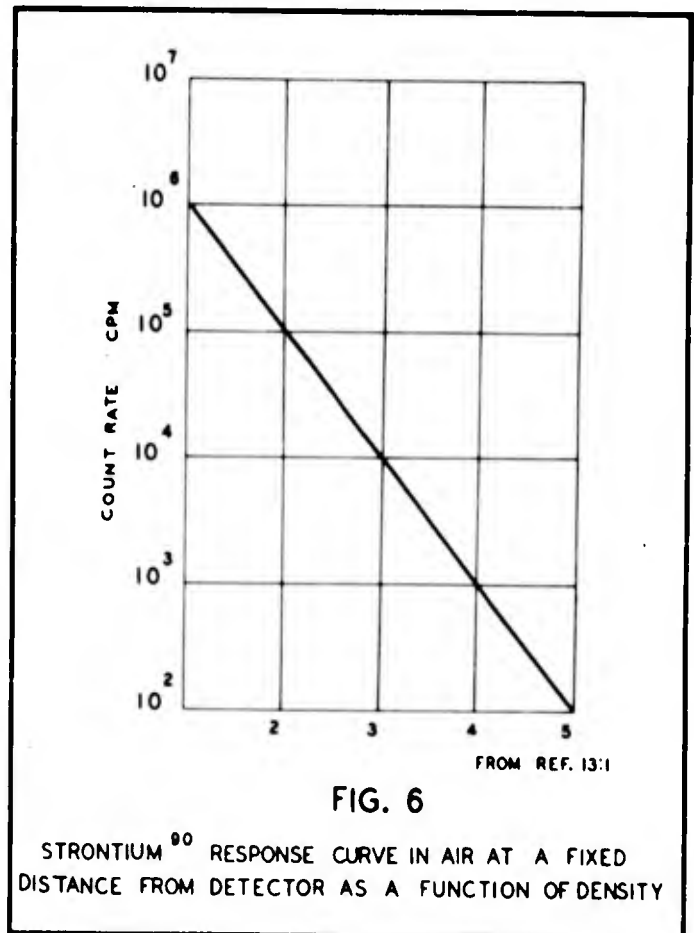
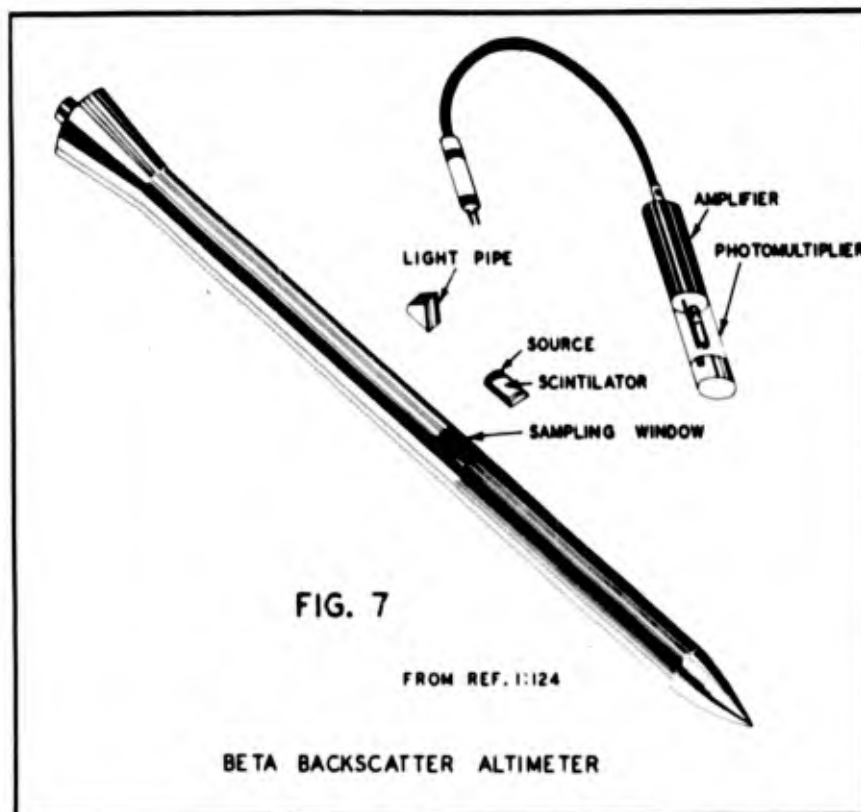


FIG. 6

STRONTIUM 90 RESPONSE CURVE IN AIR AT A FIXED DISTANCE FROM DETECTOR AS A FUNCTION OF DENSITY

The particles leave the Pm 147 source and enter the atmosphere where a series of scattering collisions of the high speed radioactive particles



and the air molecules occur. A certain small number of the particles are turned through 180 degrees by multiple scattering and then return to the detector where they are counted. As the density altitude increases, the number of air molecules decreases; hence, the probability of a 180 degree scatter occurring is reduced and the count rate declines, which is interpreted by the instrument as altitude change.

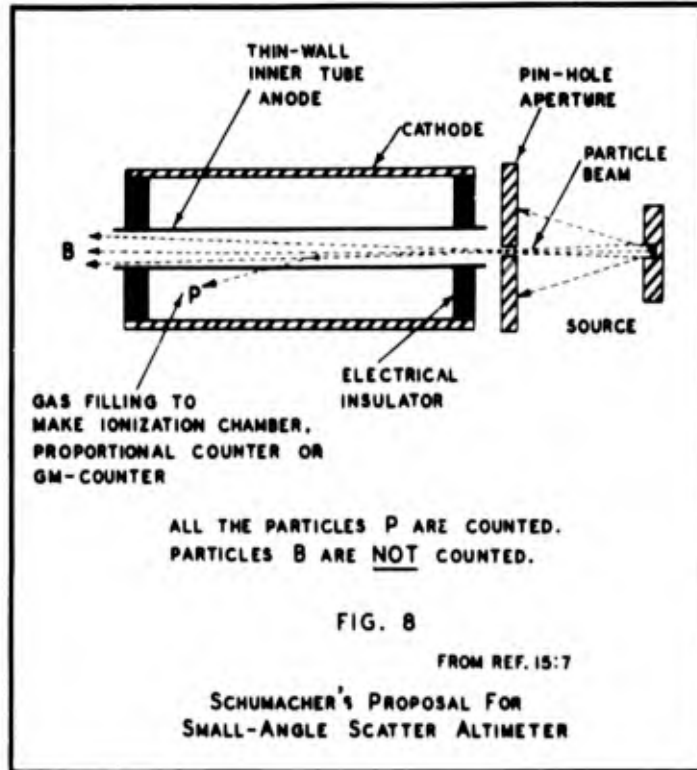
Another operational beta backscatter gage was reported on by G. Taylor of the Army Ordnance Special Weapons Ammunitions Command in a classified paper entitled, "Nuclear Altimeter," given at a

symposium at West Point, New York, in June 1962. His gage used the krypton⁸⁵ .855 Mev beta as a source and an argon filled ionisation chamber for the detector. Mounted at several points on a missile nose cone his source-detector units measured altitudes below 75,000 feet with an accuracy of 10%. Taylor mentioned that aerodynamic effects from boundary layer thickness were significant.

The principal weakness of these or any backscatter gages is the limit of detection established by the noise of the detector and electronics. In order to increase the cross section for scatter, the isotope is selected for a low beta energy (Pa 147 beta is 0.23 Mev). During the multiple collision process the electrons lose most of their energy. This requires the gain of the electronics to be kept high, which results in a high noise level; as a consequence, when the noise blocks out the signal from the returning electrons, the device no longer functions.

Small-Angle Scatter. B. W. Schumacher proposes a density gage using small-angle scatter from a beta emitting isotope which is believed will cover an altitude range to 500,000 feet or higher (Ref 15:1). The gage, shown in Fig. 8 on the following page, has two major components, the source and the detector. After the beta source radiation is collimated by a pin-hole aperture into a narrow beam, it passes down the axis of a thin walled tube which is open at both ends. The tube is the anode of an ionization chamber, proportional counter, or a Geiger-Mueller counter. Assuming that no atmosphere at all is within the tube, the beta rays will pass through the tube without striking the thin walls,

and the count rate will be zero. If only a few atmospheric atoms are present in the tube, some of the beam electrons will chance to strike



them and scatter into the tube walls. This is also shown in Fig. 8. Obviously, with an increase in the number of atmospheric atoms (or molecules) present, the number of electrons scattered and hence counted will increase as well. Since the number of atoms or molecules present in a gas is proportional to the density, the arrangement affords a simple way to measure density change through a change in count rate. Below the von Karman Line at 300,000 feet, difficulties will be encountered in feeding ambient air into the hollow tube and in avoiding boundary layer and compressibility effects. It appears that the greatest usefulness of the Schumacher single-angle-scatter gage lies in the 300,000 feet to 500,000 feet range.

Criteria and Selection of Small-Angle Scatter

In Chapter II several methods of altimetry were discussed which made use of radiations from radioactive substances. However, there remains the explanation of why the small-angle-beta-scatter altimeter was chosen to be the subject of experimental study in preference to one of the other types. The reason for this was that after comparison of each method to six established criteria, the small-angle-beta-scatter process appeared most promising for further investigation.

The criteria used were: (1) The altimeter should be light in weight, and (2) require little modification of airframe structure. (3) The range of altimetry read-out should allow use in the 100,000 feet to 300,000 feet regime. (4) Altimeter error caused by aircraft motion should be minimized; this specifically refers to errors from boundary layer, compressibility, and aircraft heating effects. (5) Changes in atmospheric composition should not be reflected by the device; only changes in atmospheric density should be recorded. (6) Lastly, power requirements of the altimeter system should be low.

The elimination procedure consisted of these seven major decisions: (1) Structural and technological difficulties accompanying the movable platform of the alpha-absorption gage eliminated it from further consideration. (2) The alpha-residual-range altimeter's inability to measure over even small parts of the 100,000 feet to 300,000 feet region made it unacceptable. (3) The large screen required of the alpha-fluorescent-screen altimeter was not adaptable to aircraft design. (4) Gamma, X-ray, and bremsstrahlung methods offered negligible

sensitivity in rarefied air. (5) Noise attending the beta-backscatter altimeters limited their usefulness to below 75,000 feet, which was not inside the altitude envelope required. (6) Experiments with beta-ray-attenuation devices showed their utility was restricted to an order of magnitude density change which is not enough, hence their elimination. (7) The single remaining method, small-angle-beta scatter, met all the criteria except that errors caused by aircraft motion were unknown, but seemed large. It was thought that collimation of the scattered radiation into a detector geometrically positioned as in Fig. 18, page 48, so that the scatter volume was outside the boundary and shock layers would minimize the aircraft motion errors. Upon this basis experimentation with small-angle-beta scatter was continued.

III. Theoretical Background for Small-Angle Scatter

Rutherford Scattering

The basic theoretical principal underlying any experiment using single-angle scatter is the classical Rutherford scattering formula:

$$D\Phi(\theta) = \frac{0.8139 z^2 Z^2}{E^2} \cdot \frac{\sin \theta D\theta}{\sin^4 \left(\frac{\theta}{2}\right)} \quad 10^{-26} \text{ CM}^2 \quad (1)$$

where

$D\Phi(\theta)$	=	differential cross section for scattering into the solid angle $2\pi \sin \theta D\theta$ with no change in velocity v
E	=	kinetic energy of the incident particle in Mev
z	=	charge of incident particle
Z	=	charge of target nucleus
θ	=	angle of scatter from incident direction

The atomic model of this formula is a point nucleus with a charge Z repelling or attracting by coulomb forces the incident particle with charge z . With electron scatter in air, z equals minus one, and Z equals plus 7.2, a weighted average between plus 7 for a nitrogen atom and plus 8 for an oxygen atom. A graphical aid for understanding

the forces and trajectories involved is shown in Fig. 9. The orbit is a hyperbola for high velocities of the electron. When the negative electron

passes close by the positive nucleus, it is attracted and turned through an angle given by Eq (1). Unfortunately, the picture is as yet incomplete, because Rutherford's scattering ignores shielding of the nuclear charge by the orbiting electrons. As a result, Eq (1) must be modified by the addition of the atomic form factor, $F(K)$ (Born's Approximation),



where $F(K)$ can be obtained from tables and graphs (Ref 2). This modification yields:

$$D\Phi(\theta) = 0.8139 \left\{ \frac{Z - F(K)}{E} \right\}^2 \frac{\sin \theta \, D\theta}{\sin^4\left(\frac{\theta}{2}\right)} \quad 10^{-26} \text{ CM}^2 \quad (2)$$

Some idea of the magnitude of the change given to $D\Phi(\theta)$ by the inclusion of $F(K)$ to account for electron shielding of the nucleus is given by the correction to the pure Rutherford Formula for scattering of 70 Kev electrons by gold atoms. For a scattering angle of 20 degrees the correction is 25% (Ref 17:279). An important point is that in general as the energies of the impinging electrons increase and as the

atomic number of the target atom decreases, the shielding effect decreases (Ref 17:279). This minimizes the error we obtain if we neglect any ionization layers in the atmosphere (D, E, and F layers). More probable than electron-electron collisions are collisions between the incident electrons and the atoms of the atmosphere (Ref 17:278) so the presence of free electrons in the ion layers is neglected and only air atoms are assumed. The Rutherford scattering is based upon atomic models, not molecular models, which means dissociation of air molecules from O_2 to $2O$ or N_2 to $2N$ has no measurable effect upon the probability for scatter.

In utilization of Eq (2), no attempt was made to integrate the energy spectrum of the isotope sources; an average energy was assumed. No corrections were made for back-scattering of electrons from the backing material of the source, and similarly isotope and self-absorption and source-window losses were not considered. Lastly, multiple scatter of the electrons in air was discounted, and it was assumed that each counted event was the result of a single scatter. The theoretical physics that attends the actual situation, which is a complicated interrelation of ranges, attenuation factors, energy losses, energy spectra, and scatter, is outside the scope of this paper; but there are excellent theoretical studies available which give the answer to some of the questions. Papers by Lewis (Ref 8) and Spencer (Ref 18) are among these. The purpose of the theoretical discussion here is merely to discover if operation of a small-angle-scatter gage with a practical count-rate return is possible within the 1000,000 feet

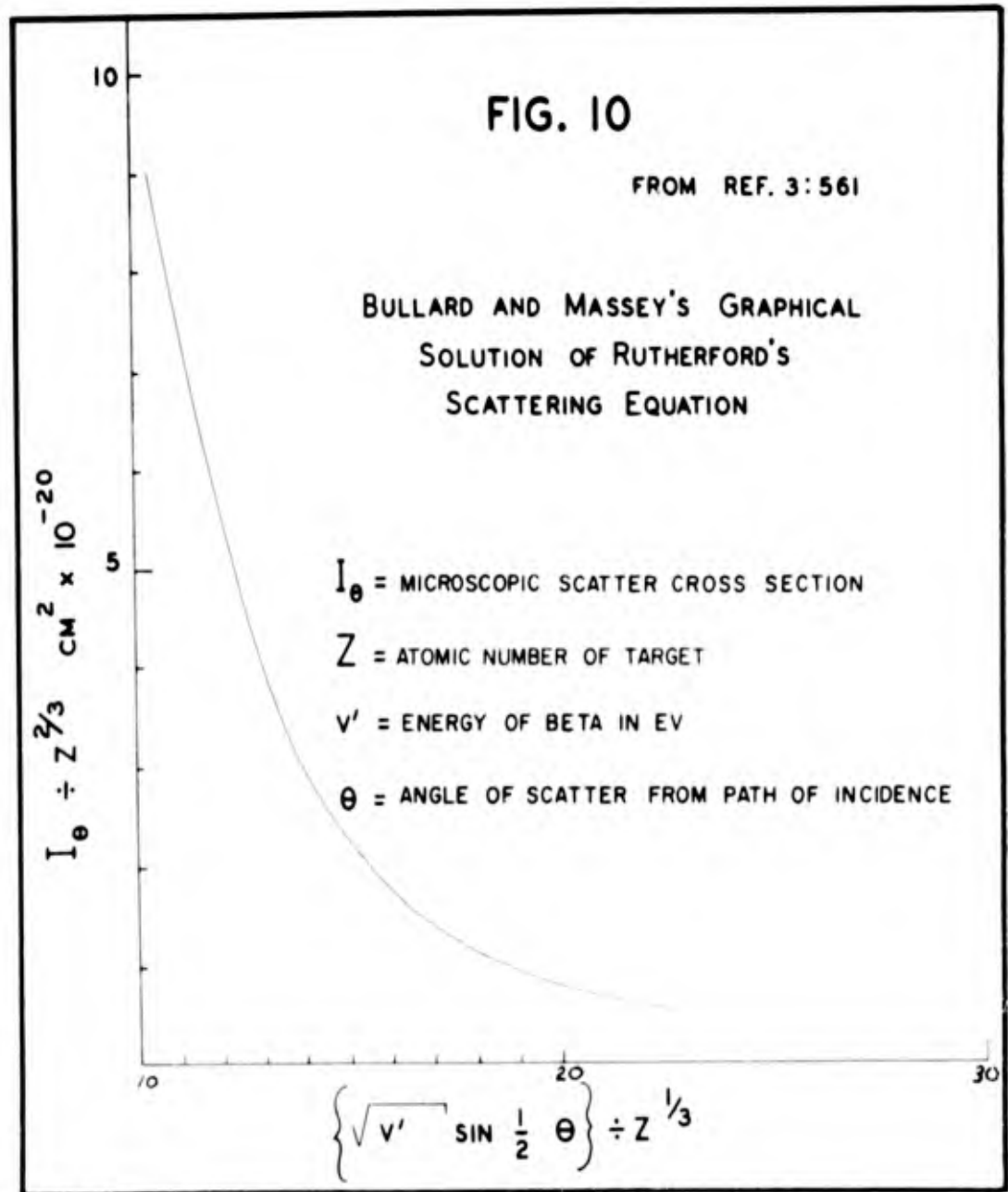
GA/Phys/62-13

to 300,000 feet altitude regime. For this purpose, the graphical solution of Eq (2) by Bullard and Massey offers a convenient tool. Their solution gives the results for all angles, atomic numbers, and velocities in a single curve (Ref 3:561) which is shown in Fig. 10 on the following page.

Theoretical Prediction of Scattering Intensity

The Bullard and Massey Curve is used to compute the theoretical results in Appendix C, which determines the counts per unit time as a function of density altitude, and this is presented in Fig. 10a, page 20. From examination of Fig. 10a and Appendix C, variables that can be changed by the experimenter are:

- a) range between source and detector
- b) average energy of emitted particles through isotope selection
- c) angle of scatter
- d) density of air.



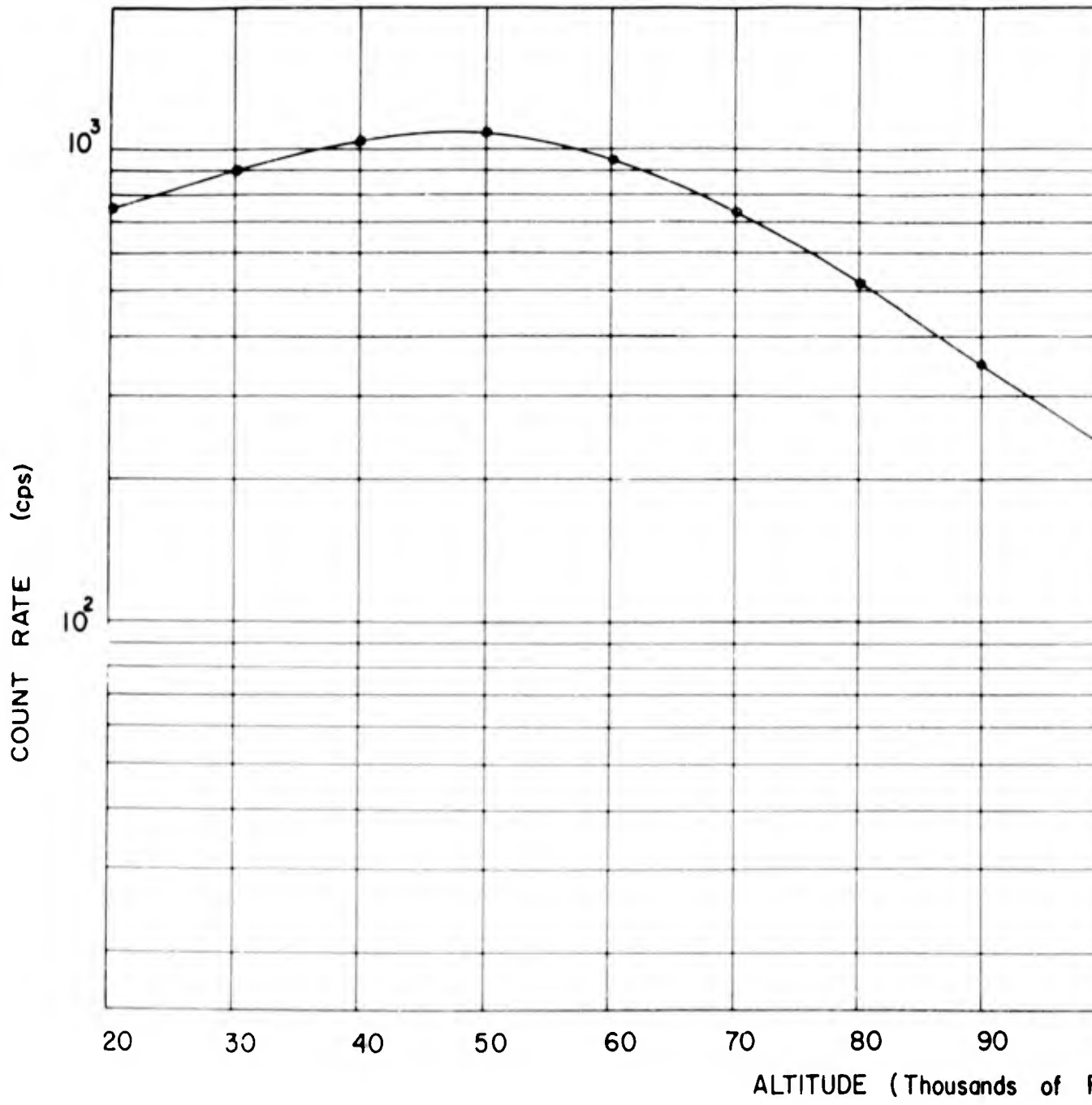


FIG. 10a

Theoretical Determination of Count Rate as a



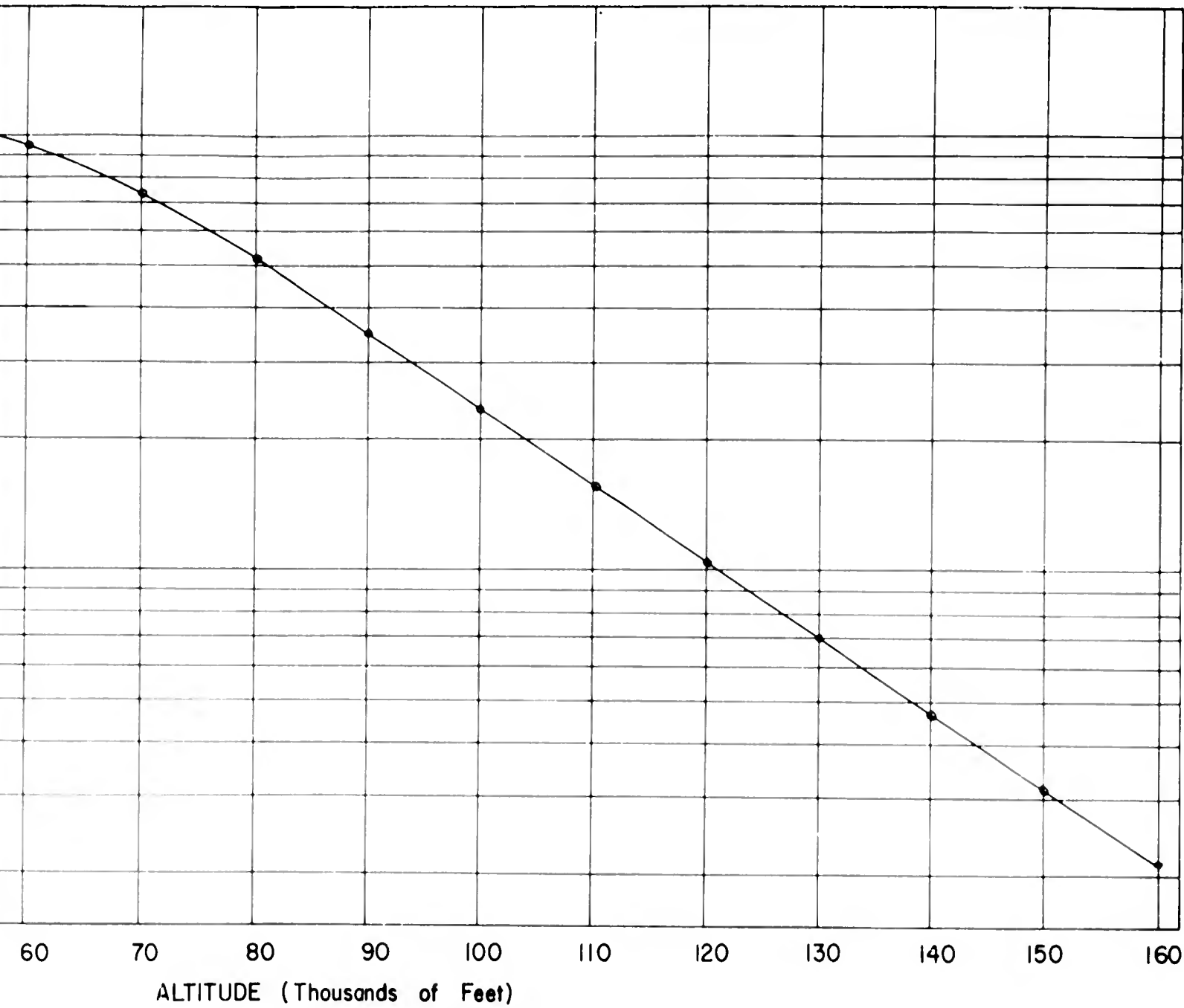


FIG. 10a

mination of Count Rate as a Function of Density Altitude

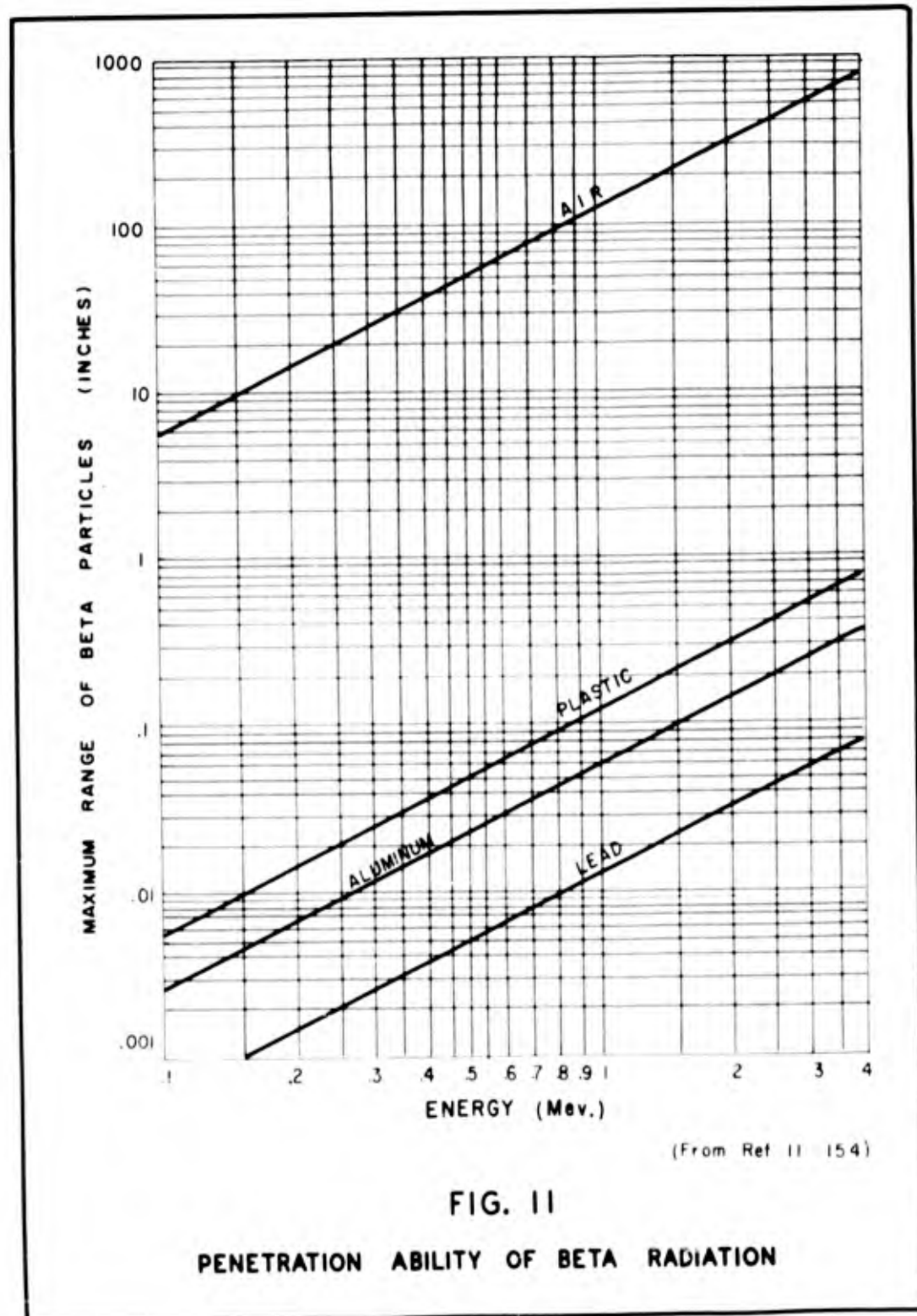
IV. Experimental Design of Small-Angle-Scatter Altimeter

Preliminary Design

This section discusses the fundamental characteristics of each component of the altimeter that most affected the early design.

Isotopes. In using radioactive isotopes, only certain energies of particles are available, and most are in the Mev range. The lower energies are desirable because the probability of scatter increases as the energy decreases. In addition, the radiological health hazard is less severe. On the other hand, beam attenuation plays a larger role in the low energy spectra, and this effect raises the lowest altitude at which the device becomes usable. Daughter decay products must also be considered. For example, if a beta emitter decays into a gamma emitter, the gamma radiation must then be shielded against or eliminated from the counting circuit in some way, since the gamma rays would otherwise decidedly affect the counting of the beta causing a high background count. Cost, half life, and availability are other factors to study with care. Cost in itself may be the determining factor in the final selection, because the price of beta emitters ranges from \$4,000,000 per curie (for calcium⁴⁵) to \$2 per curie (for cerium¹⁴⁴) (Ref 10:81 and Ref 10:85).

Source. Two major considerations influence source design: (1) the requirement for a thin window, and (2) the need for vacuum operation. Figure 11 on the next page shows that .0065 inches of aluminum completely stops all 0.2 Mev electrons, the average energy of the strontium⁹⁰



spectrum; therefore, a window of .00065 inches of aluminum permits passage of one-half the original number of strontium⁹⁰ electrons.

Vacuum operation places additional restraints upon source construction. In order to avoid the forces generated by rapid pressure changes during climbs and descents and at the same time to permit thin window construction, the isotope backing material must be pressed against the isotope. No space can be permitted between isotope and window, and the source then must be evacuated and hermetically sealed.

Source Collimator. The purpose of the source collimator is twofold: first, to collimate the beta rays into a thin beam which will allow the detector to receive small-angle scatter without direct beam interference; and second, to minimize bremsstrahlung radiation through the correct choice of material for shielding. The innermost part of the source collimator should be of low density material which gives off the least amount of bremsstrahlung, and the outermost part should be constructed of the most dense material practical in order to shield out the bremsstrahlung radiation that does occur. Failure to provide proper shielding will cause high background and reduced sensitivity from nondiscriminatory detection devices and will present serious health hazards in the case of high energy sources.

Detectors. Five main beta ray detection systems are in use today: ionization chamber, proportional counter, Geiger-Mueller tube, scintillators, and solid-state detectors. Selection of a suitable detector for use in the altimeter is determined mainly by counting rate requirements and geometric limitations of the aircraft. Energy discrimination

in the counting process, a property of the ionization chamber, is not necessary since the purpose of the detector is to record numbers of events and not energies involved. Both Geiger-Mueller tubes and proportional counters can be constructed in a myriad of shapes: needles, cylinders, parallel-plates. Placement within the structure of the aircraft should be easy, and these counters may offer the only possible solution in practice. Maximum count rate acceptance for the proportional counter with one percent loss is 20,000 counts per second (Ref 9:155). Even lower in maximum count rate is the Geiger-Mueller tube, which has a dead-time about 500 times that of the proportional counter (Ref 9:155).

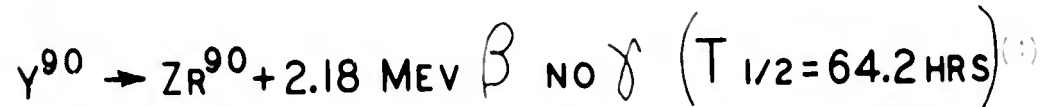
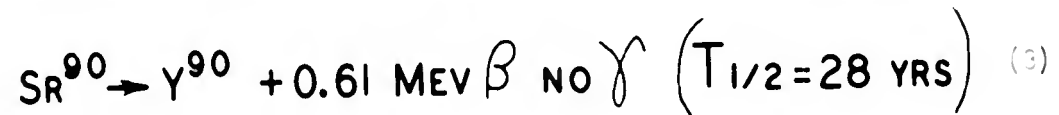
The three detection methods discussed so far have all been gas-filled chambers, which when operated in near vacua pose structural problems because of the pressure differential. This disadvantage does not exist in the next two methods. If count rates in the range of 100,000 counts per second are expected, the scintillator is a possible choice. Most scintillators have response times so short that the resolving time for the detection system is determined not by the scintillator but by the electronic amplifier or scaler. A limitation of the scintillator is its inability to detect low-energy betas, and for this purpose the proportional counter has better resolving powers, providing a thin enough window can be constructed.

Solid-state devices have now been developed to such an extent that they are, in some respects, superior to scintillators for beta spectrometry (Ref 17a:53). The semiconductor detector is essentially a

solid-state ionization chamber which in addition to linear response to beta energies has the well known advantages of all solid-state devices: small size, rapid response, minimal circuitry, and a low excitation energy (one-tenth that of gas counters).

First Experimental Design

Isotope. Strontium⁹⁰ yttrium⁹⁰ was selected mainly because of its availability in the laboratory; it is not the best choice because the high energy betas emitted reduce the probability for scatter. The decay characteristics (Ref 10:139) are:



Source. The 213 millicurie isotope³ is housed in a medical eye-applicator meant to be used for removal of cysts of the eye. It can be operated in high vacua if special precautions are observed since it is hermetically sealed in a stainless steel cylinder. Figure 12 on the following page shows an outside view of the source, plexiglass hand shield and handle, which together with a wood box with a lead and steel shield for storage are commercially available from Tracer Lab.

³Computed on 27 July 1962.

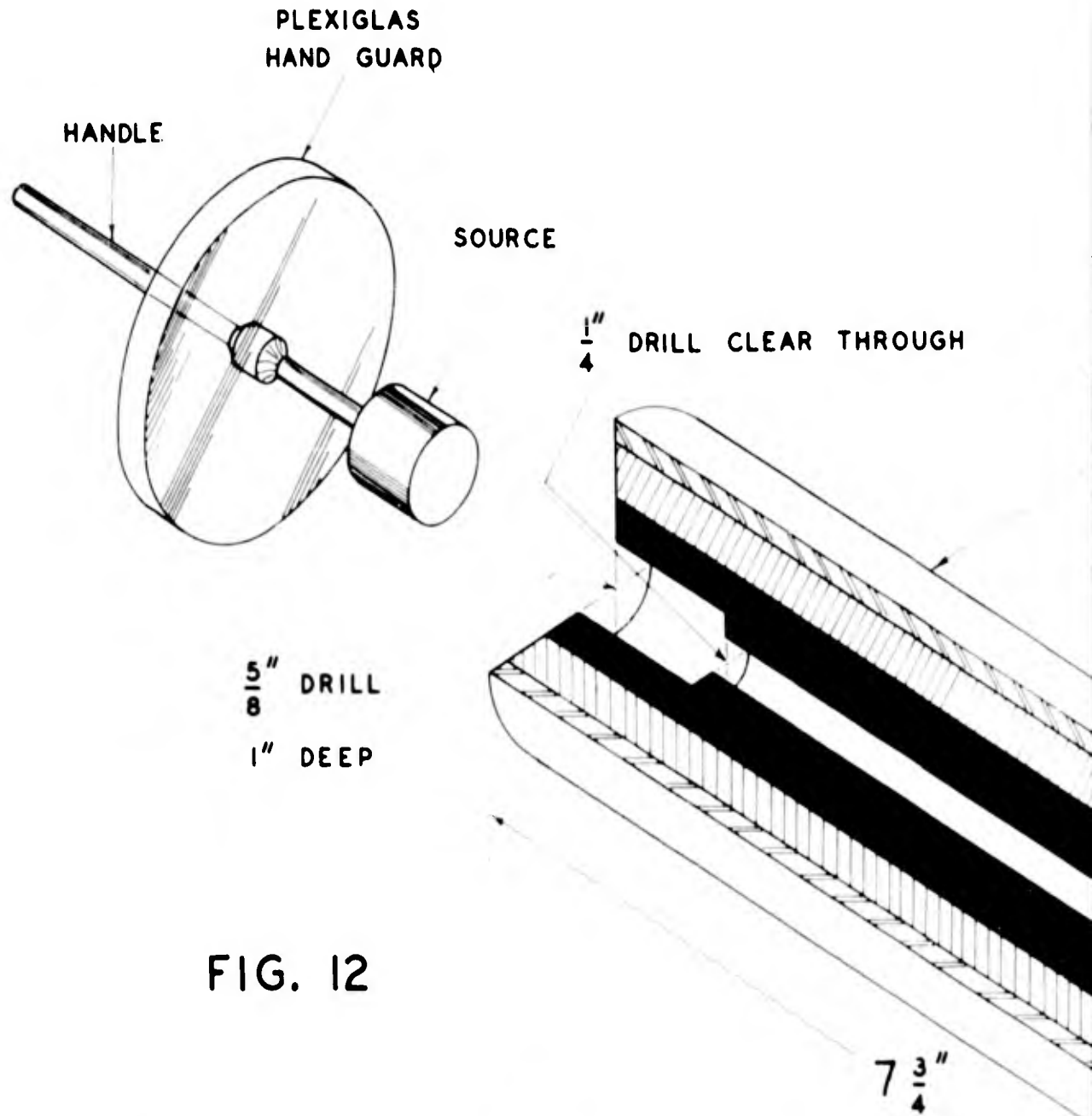


FIG. 12




SOURCE & SOURCE COLLIMATOR
(NOT DRAWN TO SCALE)

1

AS
WARD

SOURCE

$\frac{1}{4}$ " DRILL CLEAR THROUGH

LEGEND	
	IRON
	LEAD
	ALUMINUM

4" INSIDE D PIPE $\frac{1}{4}$ " THICK

$\frac{5}{16}$ " DRILL 1" DEEP

$7\frac{3}{4}$ "

COLLIMATOR OR
LE)

2

Source Collimator. A half-section view of the source collimator with dimensions and materials is found in Fig. 12. To afford shielding, the aluminum cylinder was supported in the iron pipe which was then filled with 1 11/16 inch thickness of lead. This amount of shielding would not be necessary in actual use, but was included in the laboratory design to permit long exposure to personnel at short ranges with no harmful effects.⁴ A 5/16 inch graphite plug, removed after the pouring of the molten lead was completed, provided a continuation of the center-drilled hole in the aluminum through the lead. This arrangement gave 1 inch lead shielding over the face of the aluminum collimator to protect against bremsstrahlung in the forward direction. Failure to provide lead shielding in front necessitated redesign of an earlier collimator after it was observed that changing the scatter angle from 10 to 40 degrees did not measurably affect the count rate in atmosphere. The beta scatter counts had been masked by the much higher uncollimated bremsstrahlung radiation.

Detector Collimator. Figure 13 on page 28 shows a half-section drawing of the detector collimator, which consists of two aluminum pipes, the smaller of which is concentrically supported inside of the larger by two aluminum spacers. Originally, the spacers were manufactured of cardboard; the result of this poor design is reported on page 46. Not shown on the drawing is the 1/2 inch thick, 12 inch long removable lead shield that can be placed around the outside of the detector collimator

⁴Cutie Pie measurements at the side of the source collimator read 0.7 milliroentgen per hour.

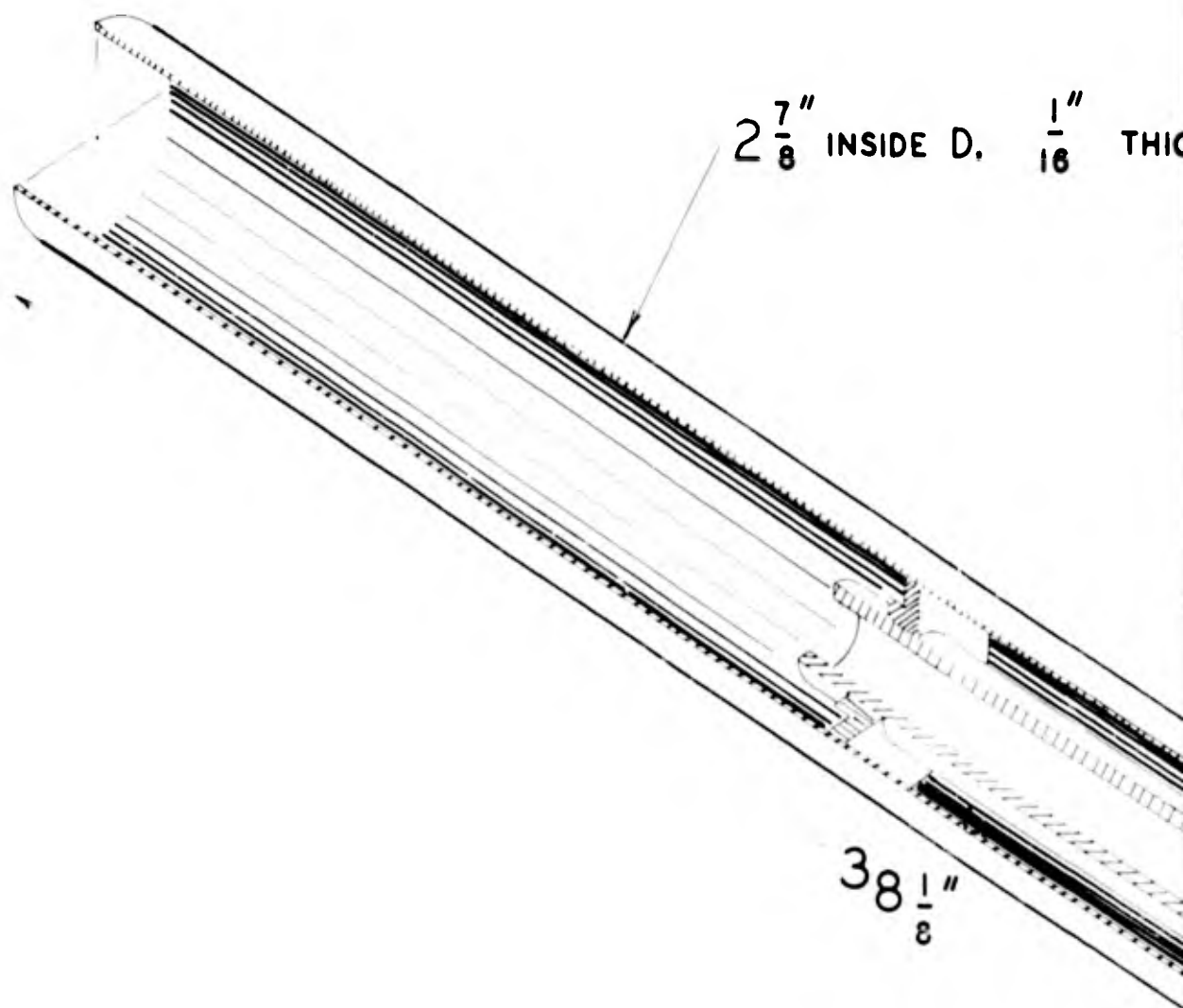


FIG. 13
DETECTOR COLLIMATOR

$2\frac{7}{8}$ " INSIDE D. $\frac{1}{16}$ " THICK

$\frac{1}{16}$ " INSIDE D
 $\frac{7}{32}$ " THICK
 $21\frac{13}{32}$ " LONG

$38\frac{1}{8}$ "

OR

in the vicinity of the crystal to protect against unwanted radiation. The purpose of the detector collimator was to limit the scattering volume to a volume containing only ambient air and to minimize the effect of aircraft boundary layer and shock wave patterns. That these effects may be considerable is indicated by Taylor's experiment (See page 10), which included 10% altitude errors attributed to the boundary layer. In addition, aerodynamic theory predicts a widening of the boundary layer with increasing altitude until in the vicinity of the von Karman Line it becomes of infinite thickness and is no longer discernible from ambient air. Detector collimation as a means to minimize the boundary layer problem experimentally reduced the count rate 17 times from the uncollimated count rate because the detected scatter is limited to that small volume in ambient air seen through the detector collimator.

Detector. The detector selected was a 1 inch diameter anthracene crystal, which in Fig. 14, page 30 is seen in exploded view with the aluminum foil reflector, light pipe, photomultiplier tube, and photomultiplier tube vacuum box. The 3.55 mg/cm^2 aluminum foil reflector provided a light tight cover over the ends and sides of the crystal, light pipe, and photomultiplier tube and was still thin enough to allow passage of beta rays greater than .048 Mev. Use of a light pipe prevented trapping of light in the anthracene and spread the light over a larger area of the photocathode of the multiplier tube (Ref 9:155). Coupling of the light pipe to the photomultiplier tube was done with Dow-Corning 200 high viscosity silicone oil, and adhesive tape was

1

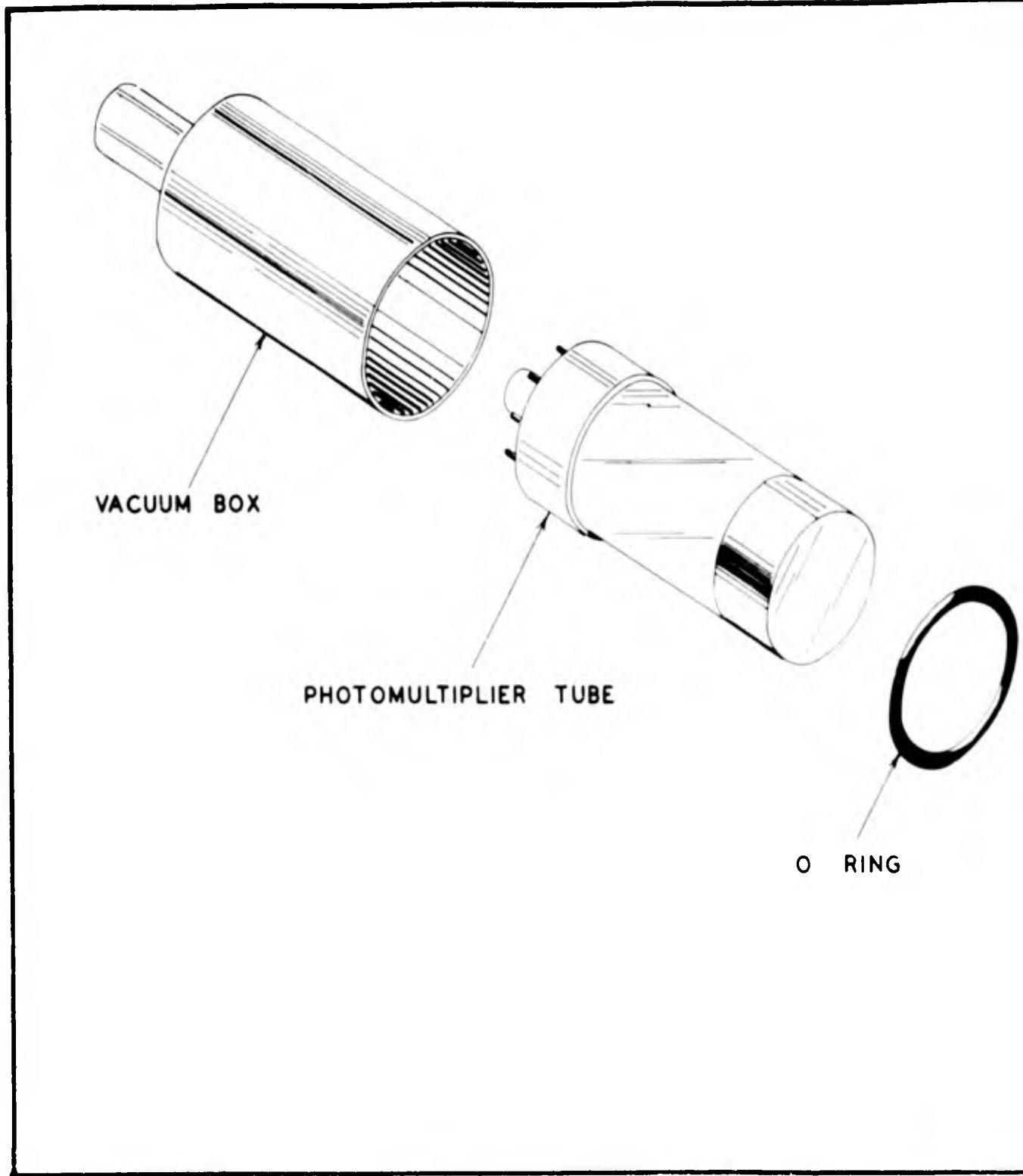
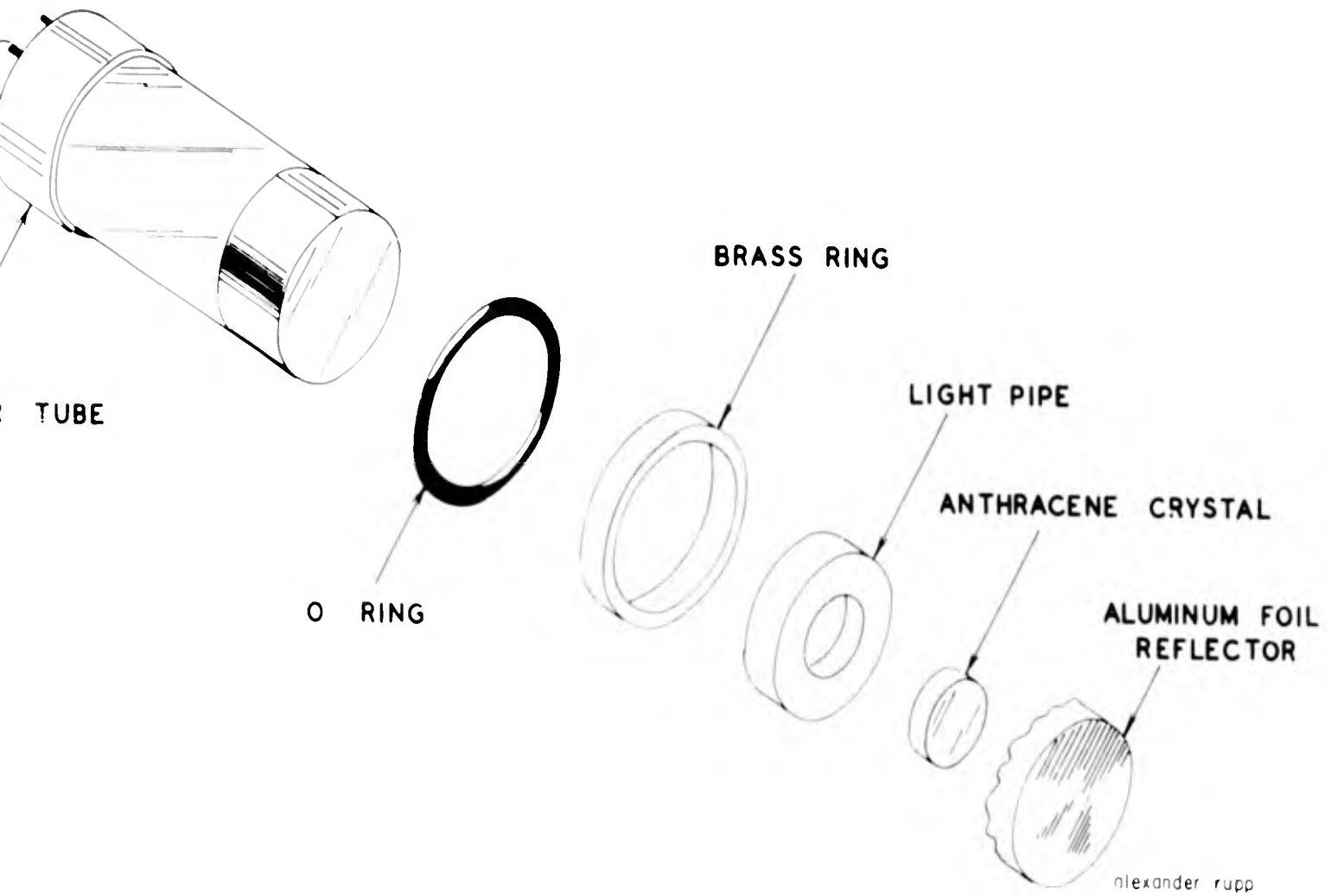


FIG. 14 DETECTOR

(SCALE $\frac{1}{2}$ SIZE)



GA/Phys/62-13

wrapped around the outside of the entire assembly to prevent slippage.

The photomultiplier tubes employed were the CBS 1002 and the Dumont 6292.

Electronics. Below are listed the model numbers and manufacturers of the electronic components used in the experiment:

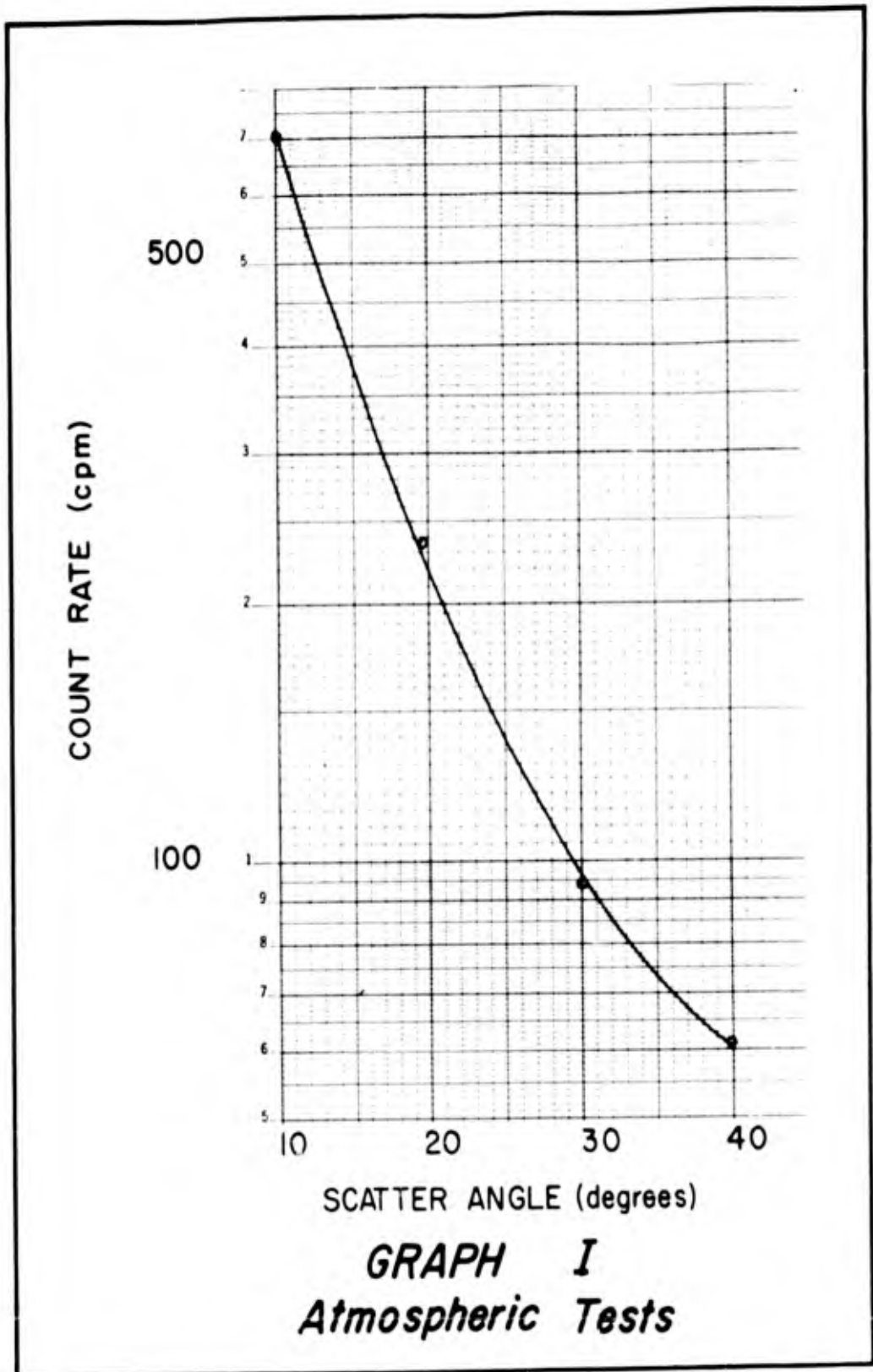
<u>Component</u>	<u>Manufacturer</u>	<u>Model No.</u>
Pre-Amplifier	Radiation Counter Lab, Inc.	A1C
Amplifier	B. J. Electronics	DA5
Ratemeter	B. J. Electronics	DM1-D
Ratemeter	Baird Atomic	412
High Voltage Supply	Atomic Instruments Co.	312
High Speed Scaler	Baird Atomic	134
Recorder	Weston	6701
Photo Tube	Columbia Broadcasting System	1002
Photo Tube	Dumont	6292

V. Testing

Initial Testing

Atmosphere Testing. The purpose of the initial atmospheric testing was to determine the effects of range and angle of scatter variations upon the count rate as well as to check the proper mating of all electronic and physical components. Experimentation always began with bore-sighting the collimators. Both detector and source collimators were mounted on optical benches which gave horizontal fore and aft travel, vertical travel, and azimuth changes. The fronts of the two collimators were first set facing each other and the distance between them was measured for range determination. With the aid of a flashlight, a man stood at the recess end of the source collimator and visually adjusted the height and direction of the two collimators until he could perfectly see the anthracene crystal target. Bore-sighting completed, the source was manually transferred into the collimator and the plexiglass hand guard was taped to the rear of the collimator. The procedure outlined here preceded all the following experiments. The atmosphere testing continued with runs at 0° , 10° , 20° , 30° , and 40° , all at minimum range to reduce the attenuation losses. Changes in count rate with the changes in angle are shown in Graph I on the following page.

Environmental Chamber Tests. The next series of experiments took place in the Environmental Altitude Chamber at Wright-Patterson Air Force Base. This extremely large chamber was chosen for early experimentation because its large size would minimize background count from backscattering



of betas from the chamber wall and the associated bremsstrahlung. Later, an experiment proved that in such a chamber, wall effects were negligible (see page 39).

The Environmental Chamber has an inside diameter of 18 feet and head-room in the center of 17 feet. Alongside is a 6 1/2 foot diameter, 6 foot long airlock. A 15 ton monorail hoist removes the top of the chamber making the entire test space of 3600 square feet available for entry. Nine mechanical vacuum pumps rated at 340 horsepower total provide the pumping system. Additional chamber facilities are electric heaters and air conditioners (temperature range is minus 90°F to plus 212°F), internal electric power, an oxygen breathing system, and innerphone communications.

Before beginning the experiments in the Environmental Chamber, it was necessary to pressure check the source to determine if it could withstand a vacuum and to determine what a safe climb rate might be. To do this, the Air Force Institute of Technology Physics Laboratory technicians built a glass chamber, a tube 18 inches long and 3/4 inch in diameter. Into one end, which was closed, they placed the source and to the other end clamped a rubber vacuum hose connected to a mechanical vacuum pump. Floodlights illuminated the source, which was observed from a safe distance through a telescope. The rubber vacuum hose was clamped in such a way that if any bulging or other sign of impending failure, or actual failure, of the source occurred, the area of contamination could be restricted to the glass container and the vacuum hose forward of the clamp. It was thought that a pressure change rate of 25 torr per minute would be

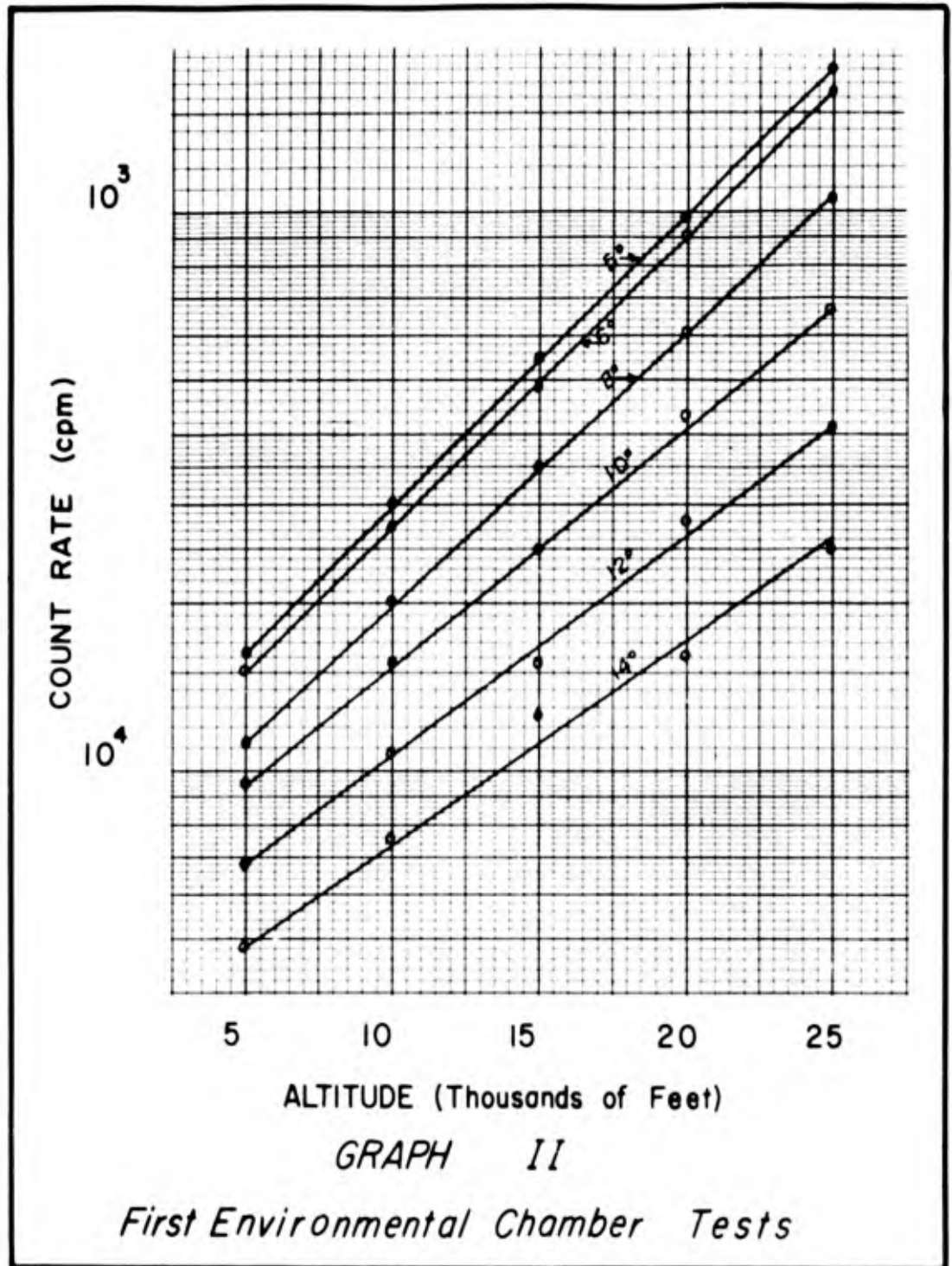
reasonable.⁵ This procedure was followed to the 1000 micron range and nothing changed in the appearance of the source. Descent was at a pressure change rate of 50 torr per minute, again with negative visual results. Wipe tests were negative as well. Accordingly, for the entire series of altitude experiments, the source was not allowed to climb or to descend at a rate faster than 25 torr per minute. Faster rates may be possible with this source; however, no tests were made to establish them.

The first Environmental Chamber test had as its purpose to find out if a measurable change in count rate occurred as a function of altitude and to determine the experimental variation of counts as a function of scatter angle. The high voltage (920 volts) arcing in the photo tube voltage divider which occurs at altitude limited these first runs to 25,000 feet, and this low altitude permitted the author, equipped with an aircraft helmet and oxygen mask, to remain in the chamber to change the scatter angles. The same experimental setup existed as in the atmospheric tests, except that now the high voltage, signal lead, and ground lead pierced the chamber wall through a nipple sealed with vacuum putty. This arrangement allowed all the electronics except the photo-multiplier tube to be operated and monitored from the outside. After optical alignment of the collimators (see page 32) at sea level, runs were performed at stabilized altitudes of 5000 feet, 10,000 feet, 15,000 feet, 20,000 feet, and 25,000 feet. The altitude pressure table used is

⁵This corresponds to an initial climb rate of 1000 feet per minute.

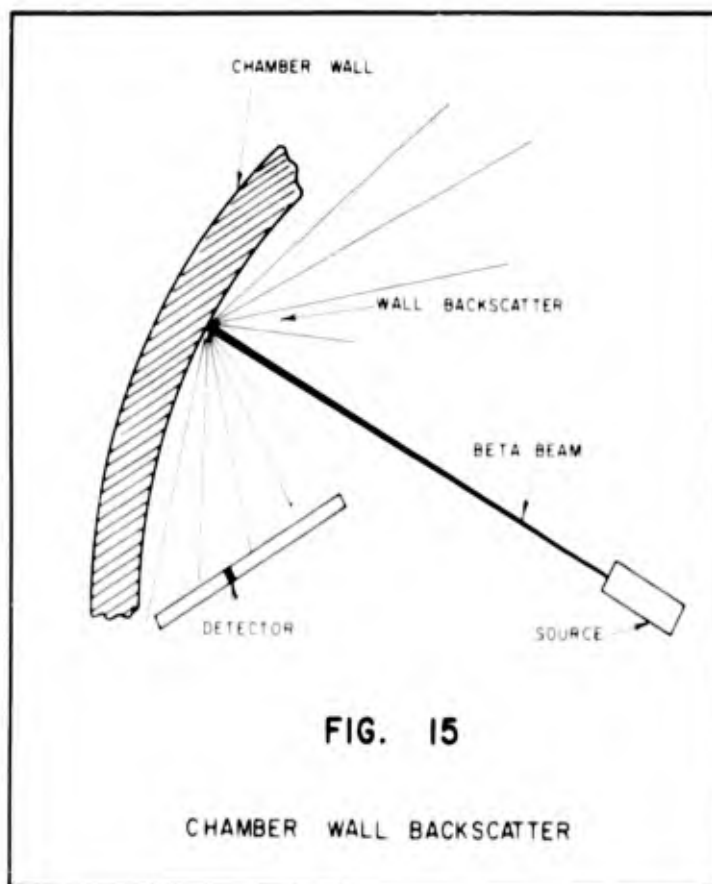
reproduced in Appendix D. At each altitude, the author manually adjusted the scatter angles from 5 degrees to 14 degrees. As predicted, the count rate change with altitude and scatter angle increases was appreciable, and the observed results are published on Graph II on the following page.

In order to reach 160,000 feet (1.08 torr), the practical limit of the Environmental Chamber, the photomultiplier tube had to be modified to avoid high voltage corona discharges at low pressures. This was done by encasing the base of the photomultiplier tube with a brass cylinder closed at one end except for a nipple, and open at the other end except for an "O" ring (see Fig. 14, page 30). Insertion of the photo tube into the brass cylinder and pulling the three (3) electrical leads through the nipple completed the modification except for sealing. The "O" ring fitted snugly around the base of the tube, and to seat the ring, a copper washer was placed inside the brass cylinder forward of the "O" ring. Then Scotch, glass-fiber-reinforced, tension tape was laid across the length of the cylinder onto the glass part of the tube, making it an integral whole. Over the tension tape black electrician's tape protected the multiplier tube from room light. Two felt gaskets fitted the brass cylinder into the outer aluminum detector collimator. Lastly, a polyethylene tube of 3/4 inch diameter connected to the nipple provided a passage for the three (3) leads out of the chamber and for the atmospheric air into the base. This allowed the base of the photomultiplier tube to be at atmospheric pressure avoiding the arcing, while the source and anthracene crystal remained in the evacuated region.



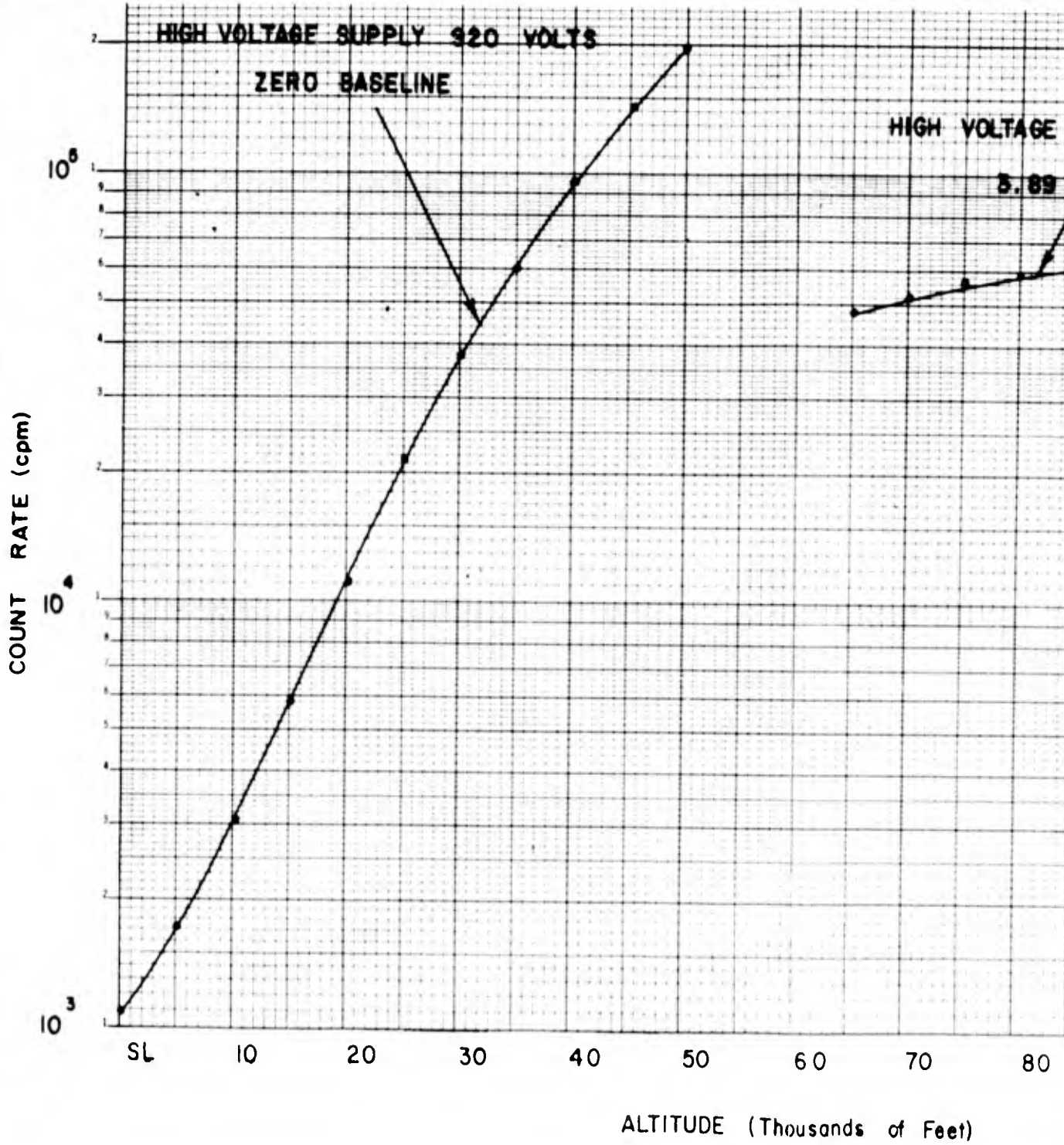
During the second Environmental Chamber test, the limit of the ratemeter count rate of 200,000 counts per minute was exceeded. In order that more data might be gathered, the high voltage input to the photomultiplier tube was reduced to lower the tube efficiency and the base line of the amplifier was increased to eliminate low voltage pulses. The results (see Graph III, page 39a), while erratic, indicated an attenuation process from 60,000 feet to 140,000 feet rather than a scattering phenomenon since the count rate increased with increasing altitude. The predicted result would be a decrease of counts with an increase in altitude. Inspection of the geometry of the source and detector showed that possibly primary beam betas were striking the end of the detector collimator causing bremsstrahlung. It was noted that after initial attenuation of the beta beam had occurred at and up to 90,000 feet, the bremsstrahlung would tend to be constant with increasing altitude, which would have the observed effect of leveling the count rate to asymptotically approach a constant value. Another possibility that had to be explored was the possibility of backscatter of beta particles from the chamber wall and the associated bremsstrahlung striking the rear of the detector; Figure 15 on the following page illustrates this. The effect of this process would also be to level the count rate after initial attenuation had occurred during the climb. To eliminate the last hypothesis, the following experiment was performed.

An aluminum target $3' \times 3' \times 1/4''$ was attached to the chamber wall in an optical line with the direct beta beam radiation. In order to protect the detector from whatever bremsstrahlung might occur, 2 inch



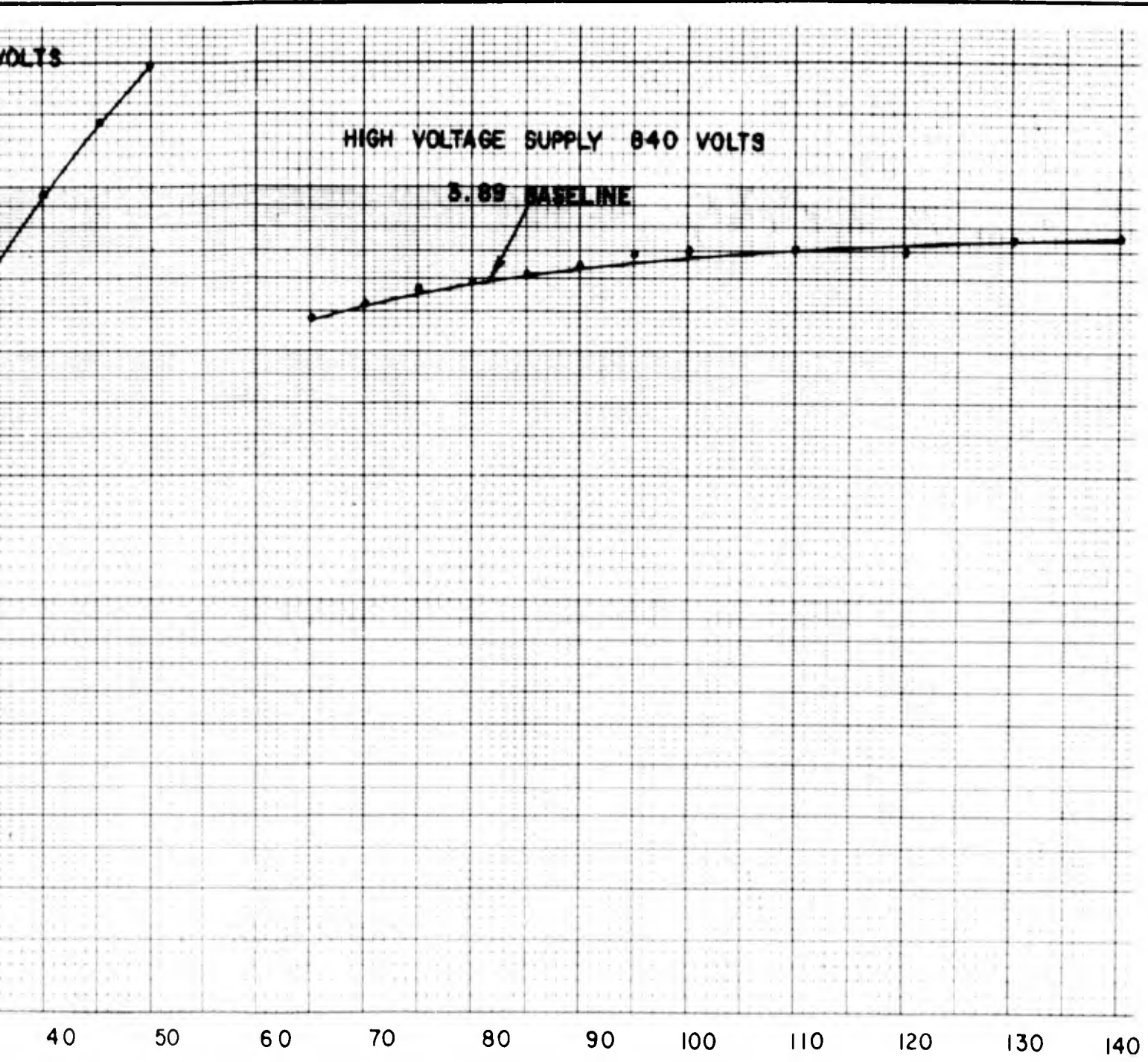
thick lead bricks were stacked in a bank to completely shield the line-of-sight from the target to the rear of the detector, as shown in Fig. 16, page 40. If the source-detector geometry was unchanged and the same altitude runs were repeated with the aluminum target and lead bricks in place, identical count-rate profiles would be recorded as before provided the wall scatter effects were negligible or nonexistent. As it turned out, the experiment showed that wall effects could be discounted.

Therefore, it was thought that fringe primary beam electrons were striking the end of the detector collimator and this impingement resulted in enough soft x-rays to mask the scattered electron counts. Increasing



GRAPH III
Second Environmental Chamber Test

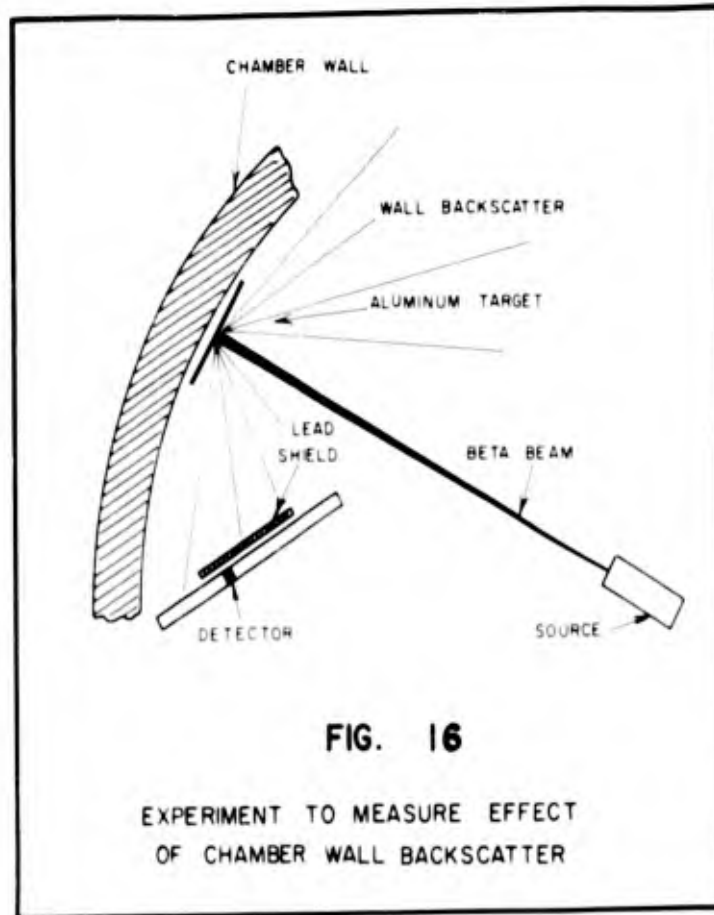
1



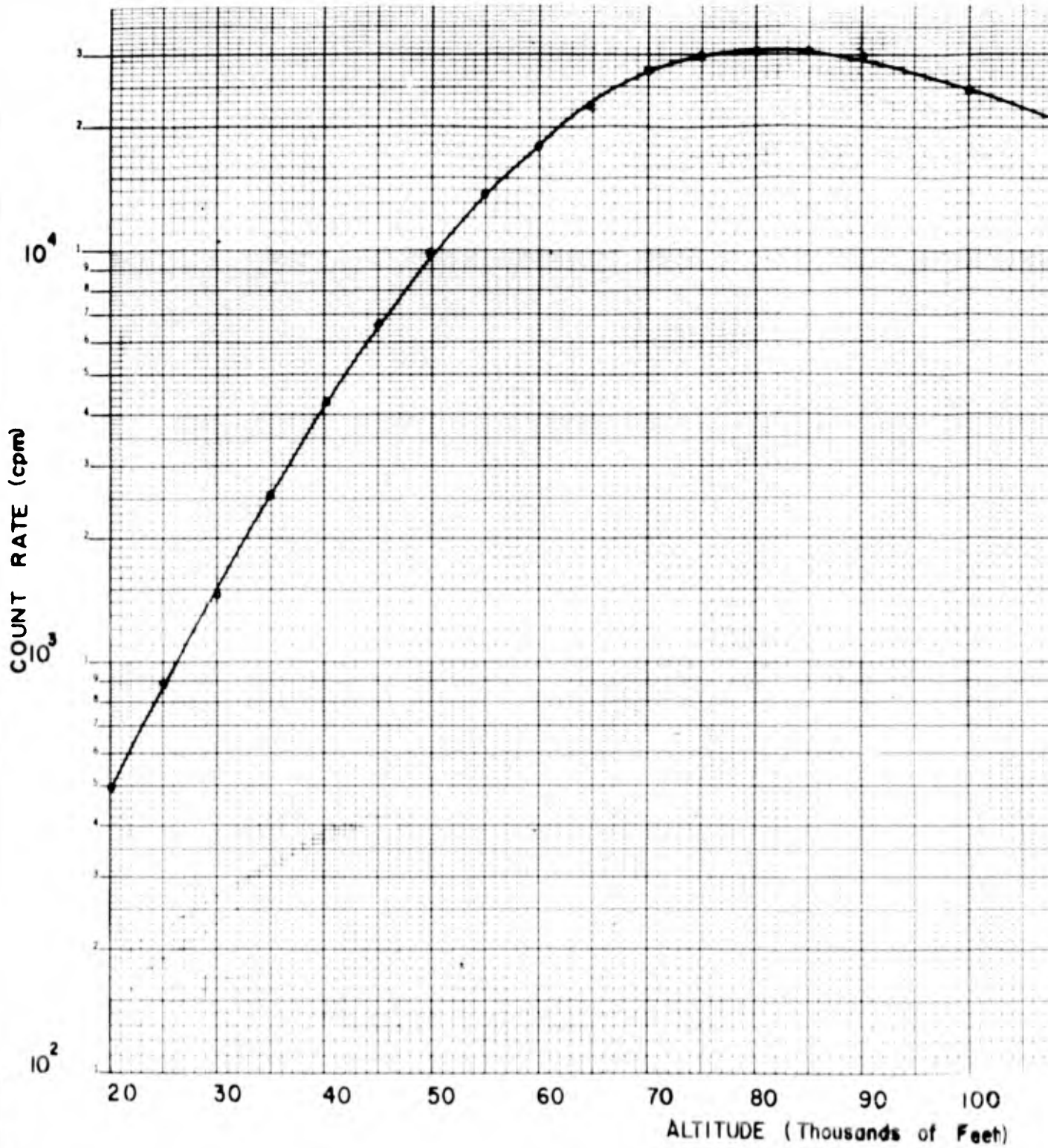
ALTITUDE (Thousands of Feet)

GRAPH III

and Environmental Chamber Tests



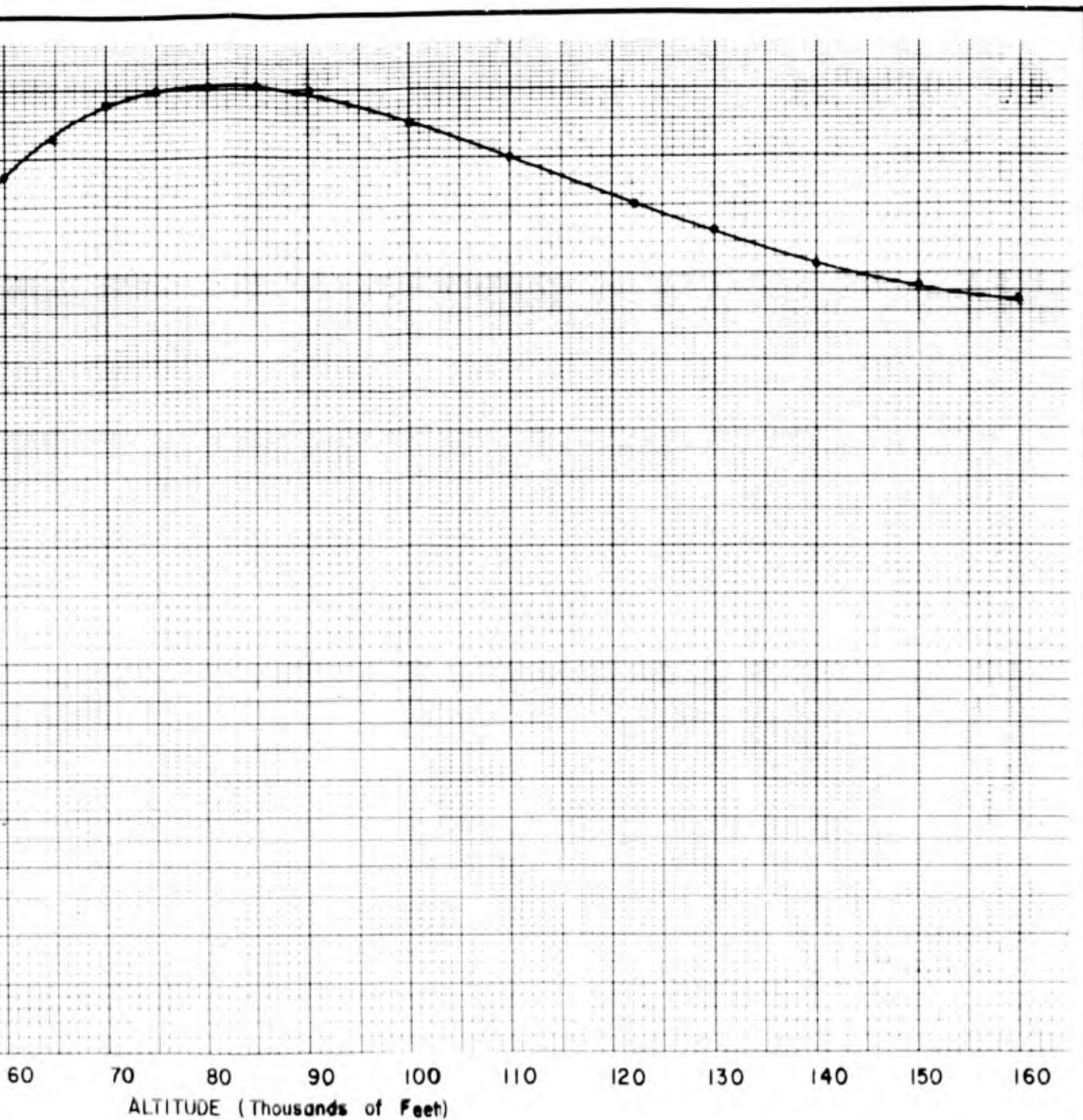
the range between source and detector and widening the angle of scatter would overcome this defect; therefore, the range between ends of the collimators was changed from 17 inches to 49 $\frac{7}{8}$ inches and the angle scatter changed from 5 degrees to 10 degrees. These improvements produced the desired result, and useful altimetry was obtained from 100,0 feet to the limit of the chamber, 160,000 feet (See Graph IV on the following page). Comparison of Graph IV, page 41, which is the actual change of count rate with altitude, to Fig. 10a, page 20, which is the theoretical change of count rate with altitude, shows reasonable similarity; and the discrepancies between the two are explained in Appendix C.



GRAPH IV

Third Environmental Chamber

1



GRAPH IV

Third Environmental Chamber Test

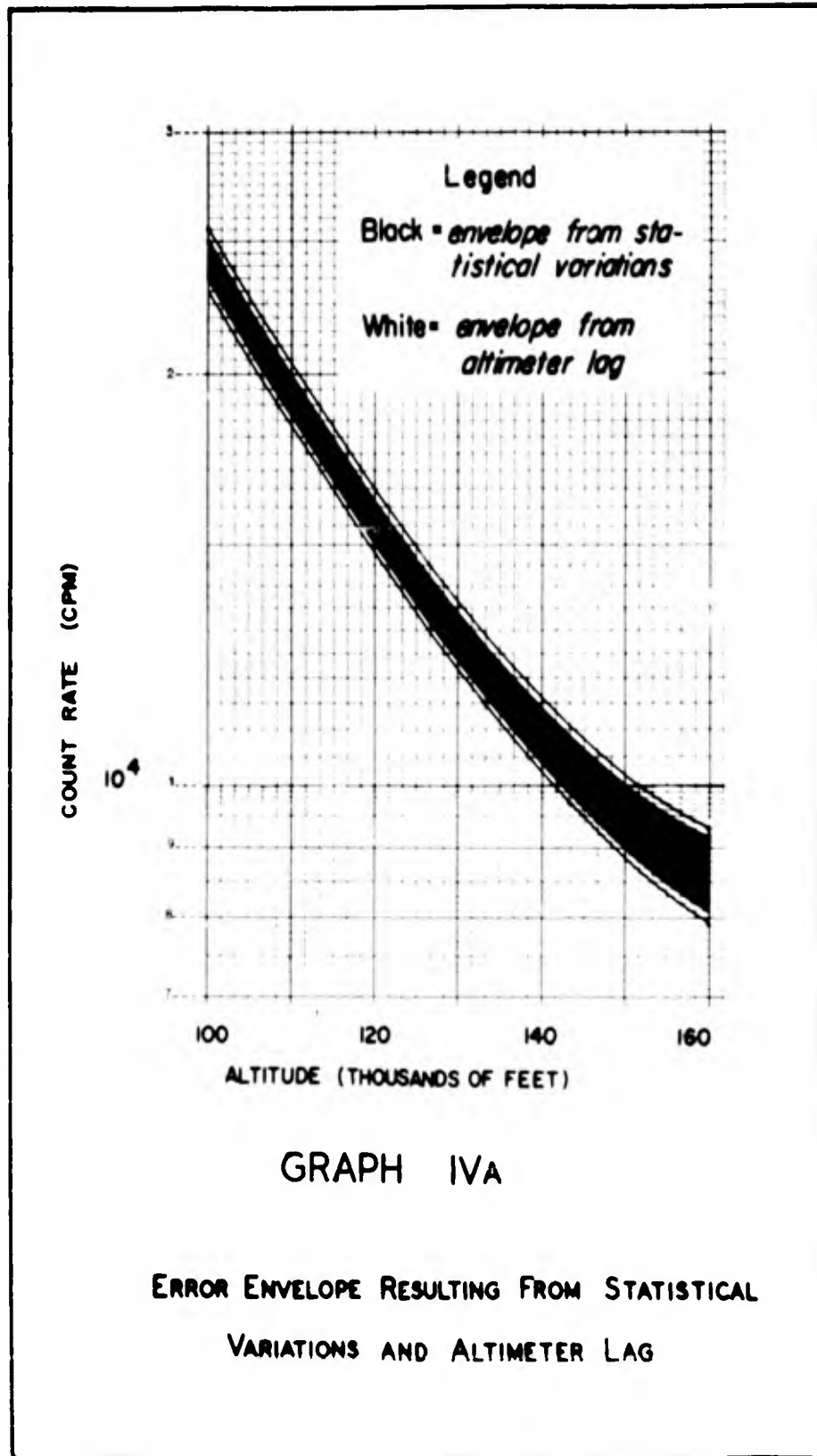
The rise in count rate during the initial climb to 90,000 feet is caused by a reduction in beam attenuation which permits more electrons to reach the scatter volume. Above 90,000 feet very little change in attenuation occurs, and the scattering process predominates. As the altitude increases and the density decreases, the number of scatters also decreases, lowering the count rate. The combination of the two processes of attenuation and scatter produces the rise and then the fall of the curve shown in Graph IV. The theoretical discussion of this curve can be found in Appendix C.

Error as a result of various climb rates and statistical fluctuations is discussed in Appendix F and is summarized for the Titan booster climb profile on Graph IVa, page 43. This total error varied from 3,000 feet at 100,000 feet to 8,100 feet at 160,000 feet, an average absolute error of 4%.

Final Design and Propulsion Chamber Tests

A much higher altitude facility than the Environmental Chamber is available at Wright-Patterson Air Force Base. The Propulsion Laboratory Chamber, an 8 foot diameter, 25 foot long tank, is used for testing ion engines in the 750,000 foot⁶ range. This extremely high altitude in such a large tank is made possible by two 32 inch diffusion pumps, a 10 inch diffusion pump, two Stokes pumps, and one Kinney pump. The facility was built in 1956 and was the first such large chamber in the world known to operate at such high altitudes. Since 1956, the chamber has been improved

⁶This corresponds to 10^{-6} torr. See Appendix E for pressure and equivalent altitudes used in the Propulsion Chamber.



with the addition of a two-stage cryogenic pump using liquid nitrogen and hydrogen. This makes possible simulated conditions up to 1,000,000 feet.⁷

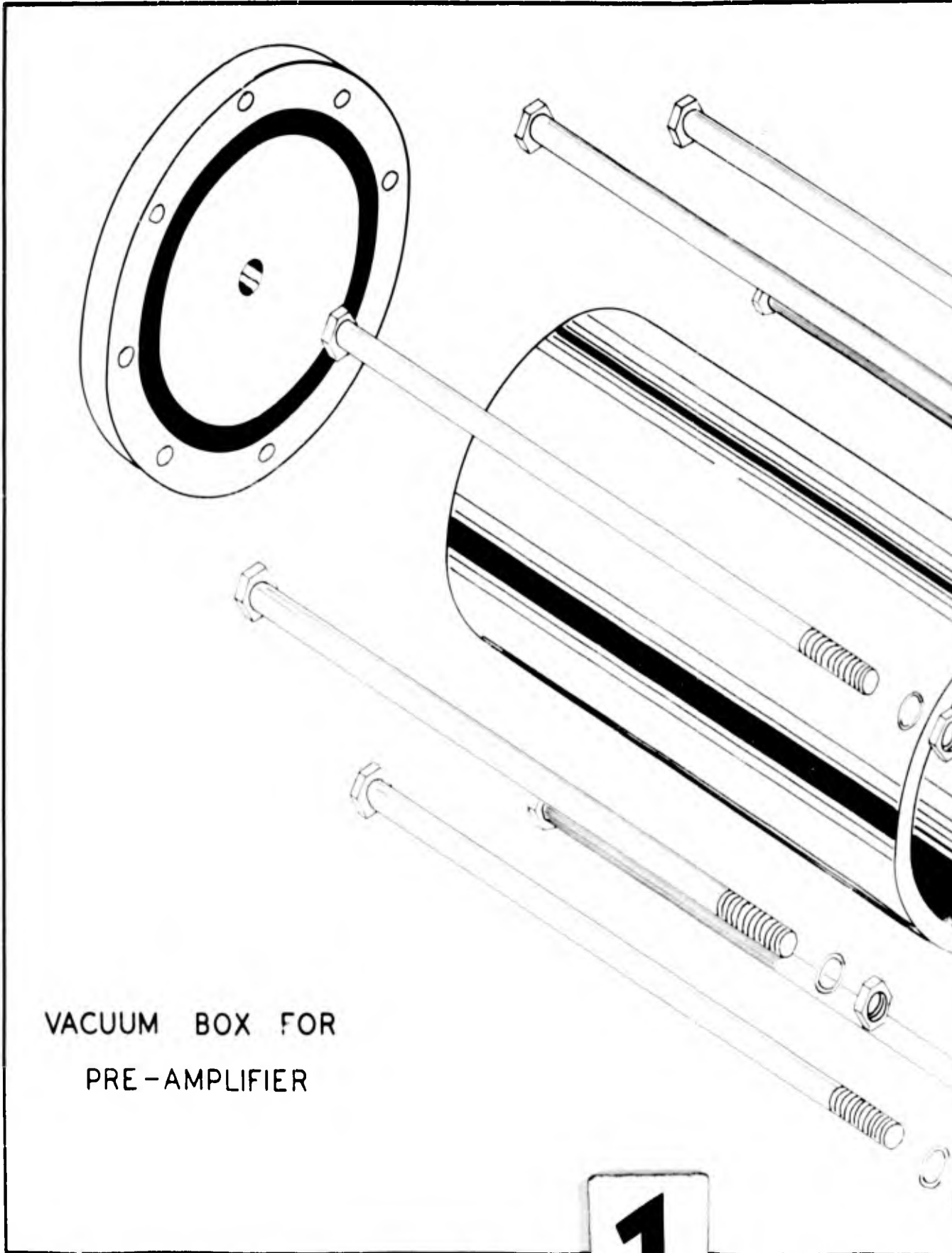
The first Propulsion Chamber run had as its purpose to determine the maximum altitude the equipment could reach without further modification. In order to adapt the equipment to the new chamber, one change was necessary: construction of a vacuum box for the pre-amp as shown in exploded view in Fig. 17, page 45. Without a complicated stand to support the optical bench near the side wall, the closest the photomultiplier tube could be to the wall outlet was 4 feet, too long a distance for the unamplified tube signal to travel without unacceptable line-loss. This long distance was avoided by manufacturing the vacuum box for the pre-amp, placing it in series with the vacuum box for the photomultiplier tube base, and supplying atmospheric pressure air to both the pre-amp and the tube in the chamber. Three-fourths inch inside diameter tygon vacuum hoses were used as connectors and passageways for the high voltage, signal, and ground leads. Otherwise the equipment remained the same as before.

During the first Propulsion Chamber run, difficulty was experienced in comparing vacuum readings taken from a McCloud gage and a Phillips gage. The Phillips gage consistently gave a much lower reading than the McCloud gage at pressures below 1000 microns;⁸ hence, it was not definitely possible to establish the chamber altitude. In order to

⁷Corresponds to 10^{-7} torr.

⁸1000 microns Hg equals 1 torr.

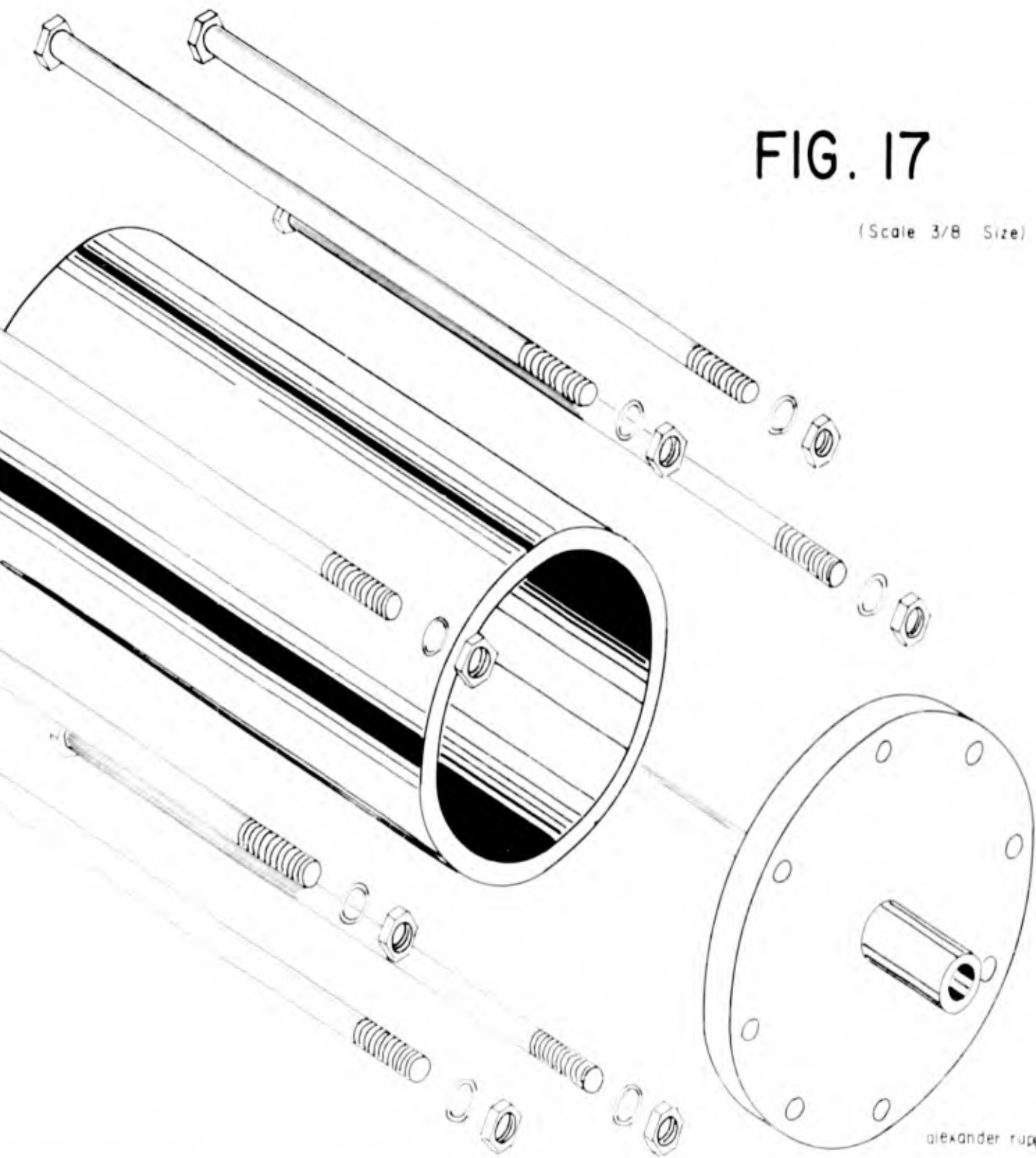




VACUUM BOX FOR
PRE-AMPLIFIER

FIG. 17

(Scale 3/8 Size)



obtain quantitative data, however, pumping was allowed to continue until at a pressure of 50 microns (measured on the McCloud gage), a sharp clear blow on the side of the chamber was heard and simultaneously all pressure instruments showed a sudden increase. The chamber personnel visually determined by means of chamber portholes that the detector collimator had blown apart. The source appeared intact, but the four-pound inner aluminum collimator lay on the floor approximately 15 feet opposite the still intact outer collimator, and the glass taped portion of the photomultiplier tube was imbedded in the wires of a conical cesium collector (part of an ion engine apparatus). A rush of air into the chamber could be heard, and it was observed that the multiplier tube vacuum box had been blown out the rear of the outer detector collimator and was hanging down supported by the tygon connecting tube.

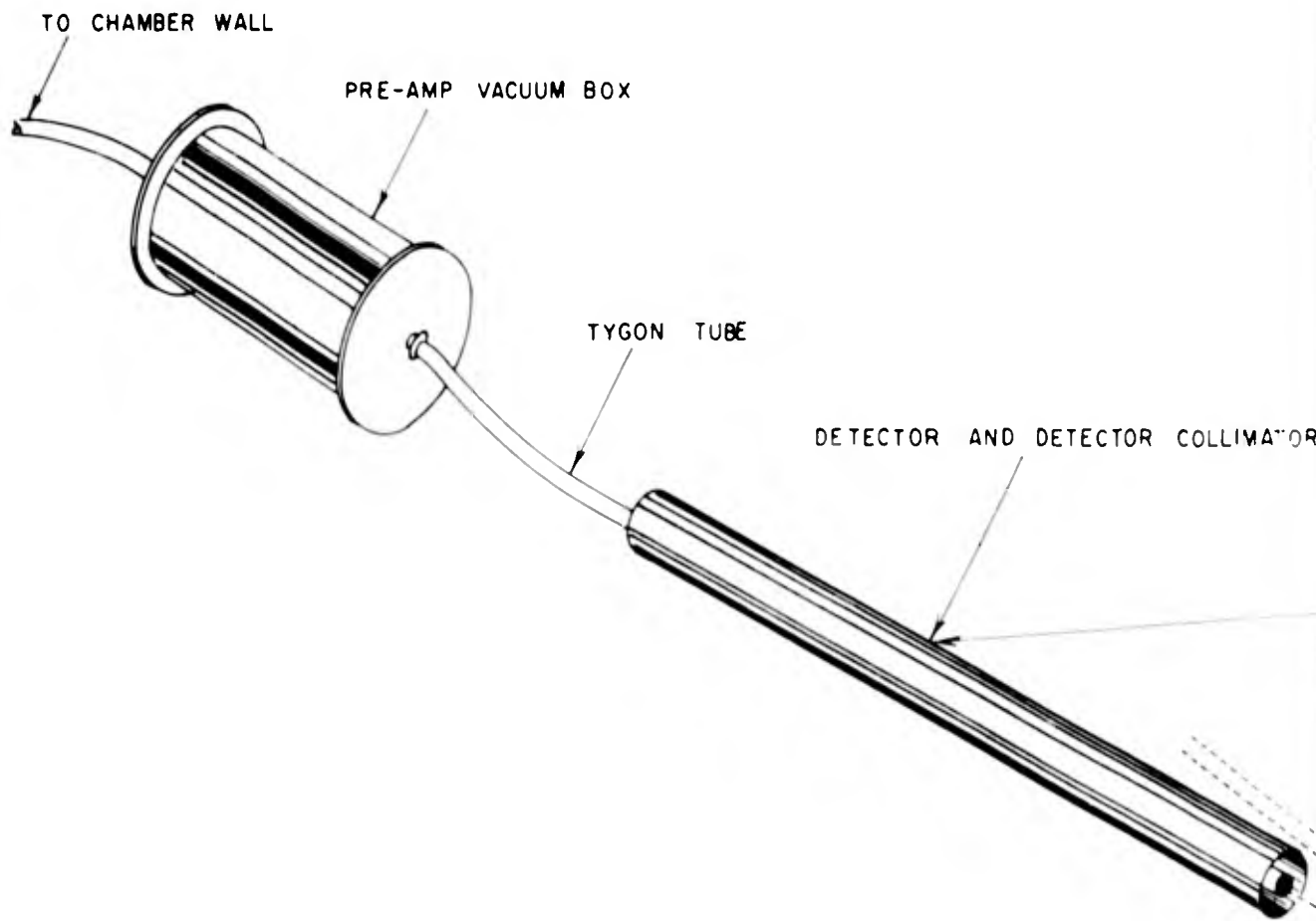
Radiological tracer equipment showed no area contamination outside the chamber or in the pump oil sumps, and had contamination existed inside the chamber, the flow of intake air during descent was thought to be sufficient barrier to prevent outside contamination. Normal descent was completed in about 45 minutes. Examination of the chamber door sill, floor, and the source holder and optical stand showed no unusual radiation. Removal of the source from its recess was effected. Wipe tests of the source window, sides, and back were negative.

Reconstruction of events showed that under a high vacuum, probably 10^{-4} torr (the McCloud gage was proven inaccurate during later experiments), the tension tape securing the photomultiplier glass enclosure to the brass vacuum box had broken under a force of 104 pounds. The

atmospheric air behind the tube then propelled the glass portion forward, and the base backward, so that the anthracene crystal and light pipe butted against the inner detector collimator. In turn the inner collimator, held in the outer collimator by unsecured cardboard spacers, became a projectile aimed by the outer collimator and shot across the chamber striking the wall 15 feet distant.

This failure necessitated a corrective redesign of the vacuum box and inner collimator. The brass seating ring was fastened to the vacuum box by four screws and the "O" ring was forced up against the phenolic of the photomultiplier base to complete the reinforcement. The final construction is shown in Fig. 14, page 30. In the event that this arrangement should also fail at the phenolic "O" ring innerface, the inner aluminum collimator was secured by metal spacers and screws to the outer collimator which in turn was rigidly attached to the optical bench. The final assembly is pictured in Fig. 18 on the following page.

Outgassing errors caused by the rubber vacuum hose of the McCloud gage made it unreliable below 1000 microns Hg. Complete reliance was then placed in the Phillips gages with sensors inserted directly into the chamber. An unexpected level off in count rate occurred at 175 microns mercury, and further pumping of the chamber to the 10^{-5} mm range resulted in no change in count rate (See Graph V on page 49); hence, the effective upper limit of these components was about 210,000 feet. A repeat experiment, identical but without the detector collimator encasing the photomultiplier tube, resulted in the same shaped count rate profile elevated sizably in magnitude with the same level off point



*Assembly for Final Small-Angle
Beta Scatter Experiment*

FIG. 18

(Scale 1/8 Size)

BOX

TYGON TUBE

DETECTOR AND DETECTOR COLLIMATOR

RANGE (SOURCE TO DETECTOR) 78"

SCATTER VOLUME

PRIMARY BETA BEAM

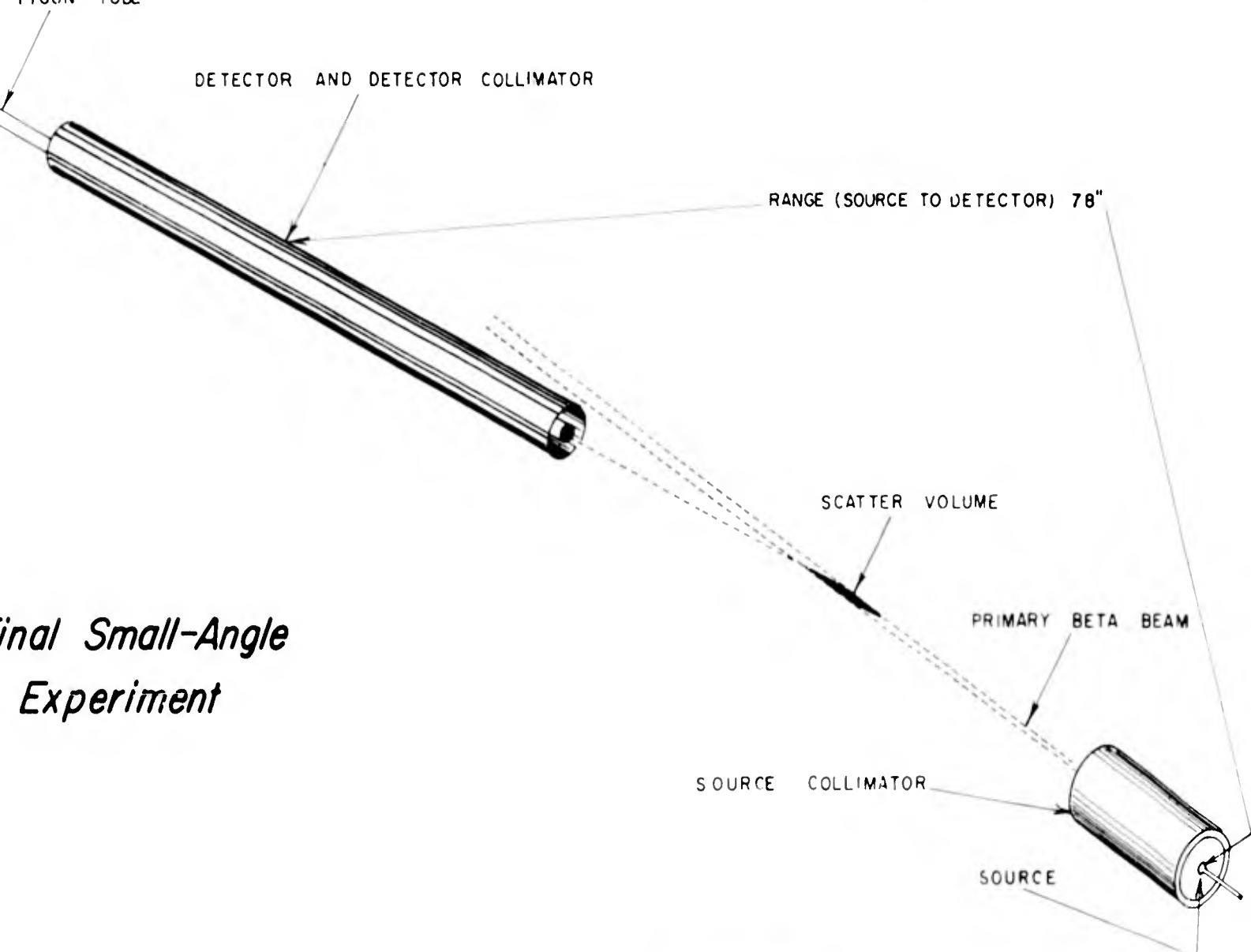
SOURCE COLLIMATOR

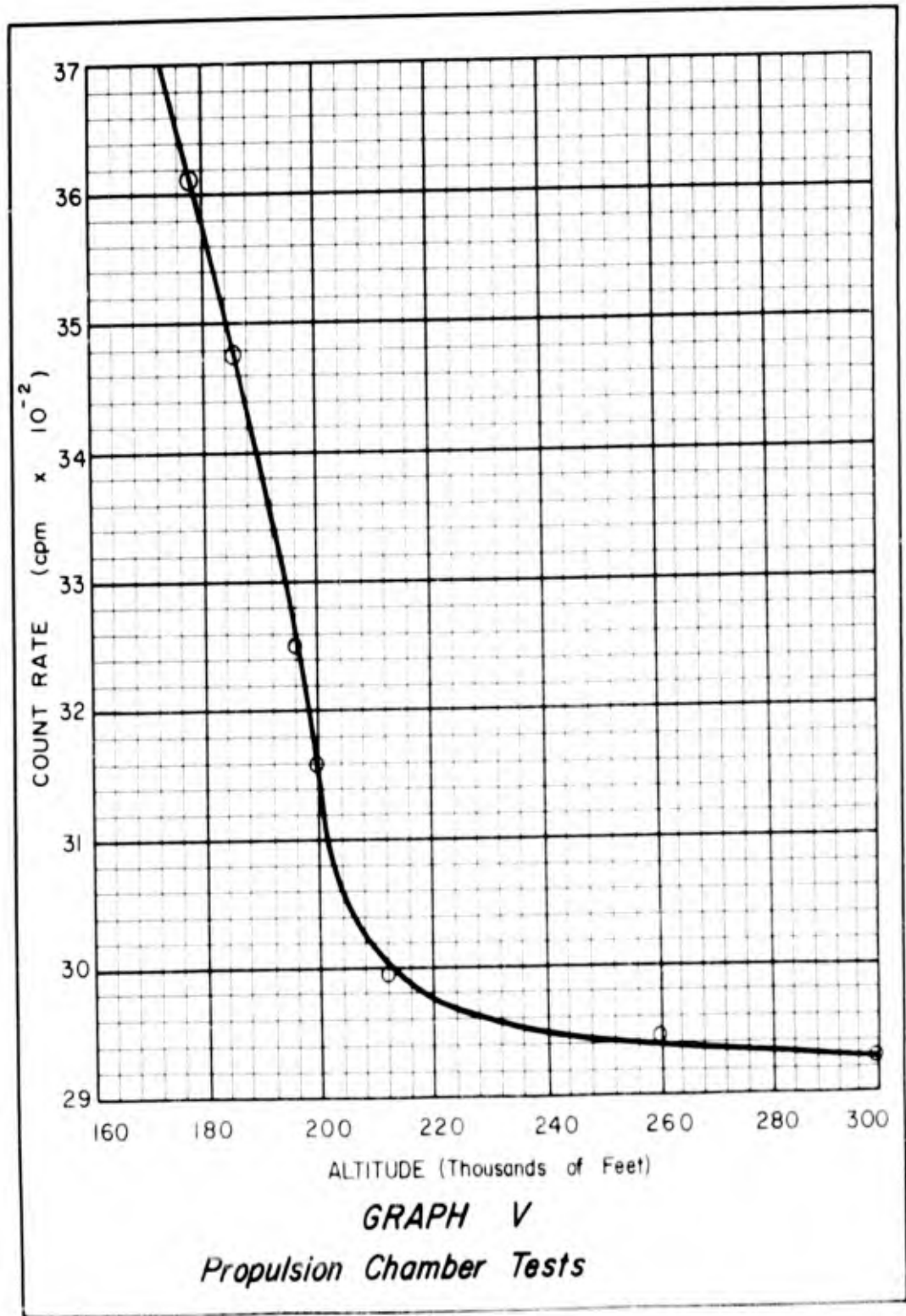
SOURCE

*Final Small-Angle
Experiment*

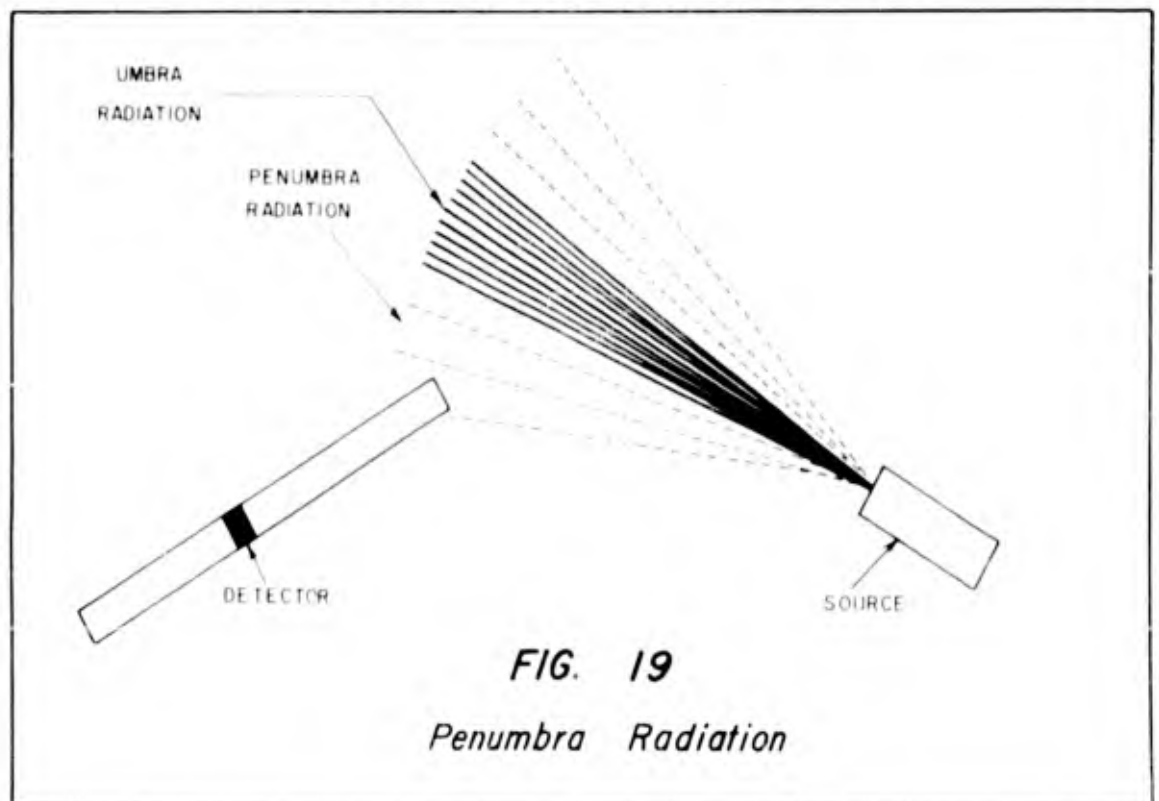
okr

2

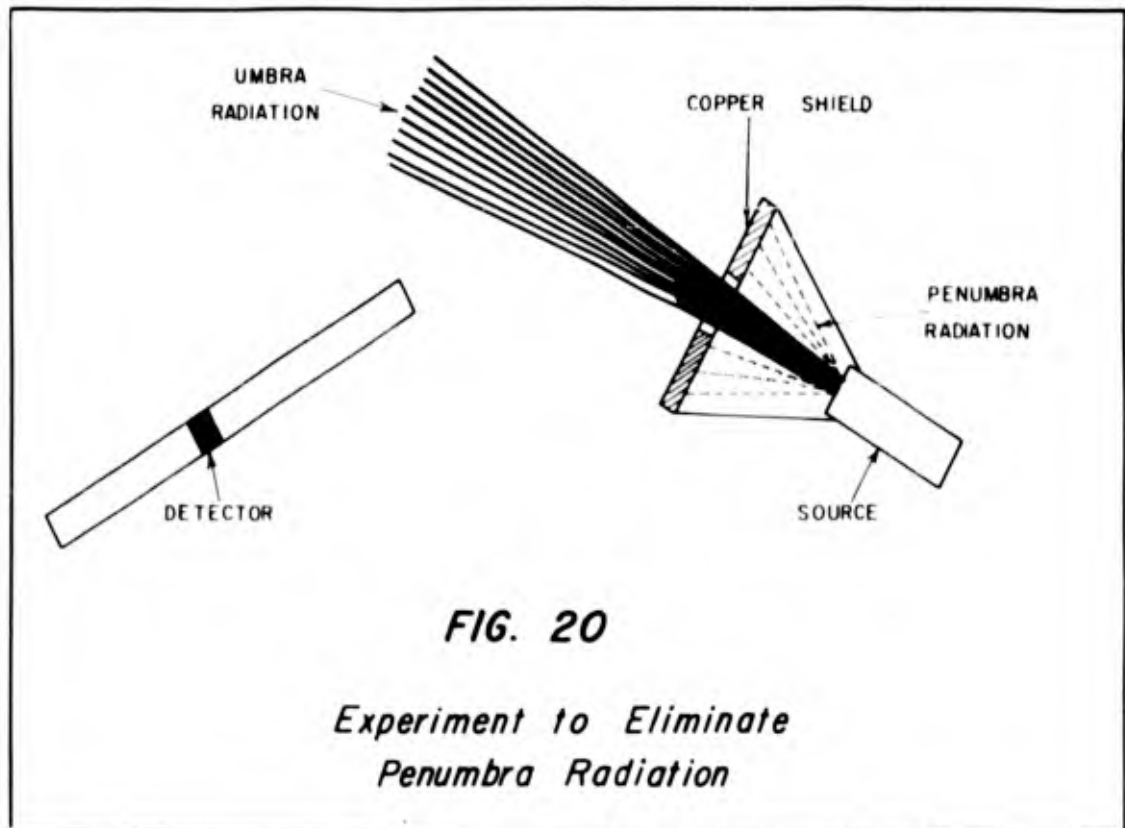




at 175 microns Hg. To determine from which direction the constant radiation at 175 microns Hg and below was being received, two additional experiments were performed. The first experiment used an aluminum target in front of the chamber wall and lead screens protecting the rear and sides of the detector, and this showed no change in count rate from the previous run. Lead bricks placed in front of the detector with the sides and rear unprotected showed a steady zero count rate at all altitudes; thus, the combination of the two experiments proved the radiation was frontal. Since the unwanted radiation was markedly affected by air attenuation at lower altitudes, it indicated beta, not bremsstrahlung, radiation. It was hypothesized that a direct beam low energy penumbra existed outside the primary or high energy umbra beam of beta radiation, which was attenuated at lower altitudes but strong enough at 175 microns to mask the scattered electrons from the main beam.



In order to check this possibility, a copper shield was built which could be used to transmit the direct beam while at the same time block the penumbra beam (See Fig. 19 on the preceding page and Fig. 20 below).



The Propulsion Chamber was not available for this test, and the investigation for penumbra radiation has not been completed.

VI. Summary of Important Results and Conclusions

After a review of all known methods of obtaining density altimetry from devices utilizing radiation from radioactive substances, the small-angle-scatter of beta particles from the atmosphere was considered as being most promising for experimental study. The completed beta-scatter device, shown in Fig. 18, page 48, provided altitude information from 100,000 feet to 210,000 feet as demonstrated by tests in the Environmental Chamber and the Propulsion Chamber and as recorded on Graph IV, page 41, and Graph V, page 49. The theory did not predict the leveling of the count rate that occurred at 210,000 feet (175 microns), and if the reason for this phenomena could be determined and the leveling eliminated, extrapolation of Graph V shows the beta scatter device to be capable of measuring altitudes in excess of 300,000 feet. The penumbra radiation hypothesis for this phenomenon has been suggested as well as experiments to validate this hypothesis.

In conclusion, it is stated that: (1) The beta scatter gage has been experimentally demonstrated feasible as a density altimeter to 210,000 feet. (2) Theoretically for a Titan boost mission the altimeter will indicate an average 4% absolute error in the 100,000 to 160,000 foot range. (3) The experimental design, modified with miniaturization of electronics, is deemed applicable for aircraft installation. (4) The device is velocity and temperature independent, but the effect of boundary layer thickness and shock wave fronts upon the final count rate is not known. (5) The design has included detector collimation in order

GA/Phys/62-13

to sample ambient air and minimize the boundary layer and shock front effects mentioned above. (6) Probes and location of the device in the re-entry high temperature areas are not necessary; the device may be located in the fuselage or other relatively low re-entry temperature area. (7) Experimentation with a higher strength source as well as a source with a lower energy spectrum seems to be a logical continuation for development. Specifically, a 2 curie strontium⁹⁰ source and a promethium¹⁴⁷ beta source ($E_{\max} = .22 \text{ Mev}$) are recommended. Consultation with aeronautical and electrical engineers for an experimental design to be tested on a rocket nose cone or an X-15 aircraft is suggested.

Bibliography

1. "Beta Backscatter Measures Altitude." Nucleonics, 18, No. 3: 124 (March 1960).
2. Betre, H. A. "Zur Theorie des Durchganges schneller Korpuskularstrahlung durch Materie." Annalen der Physik, 5:325-400 (1930).
3. Bullard, E. C., and H. S. W. Massey. "Remarks on the Scattering of Electrons by Automatic Fields." Cambridge Philosophical Society Proceedings, 26:556-563 (1930).
4. Dineff, John, et al. "X-ray Instrumentation for Density Measurements in a Supersonic Flow Field." Technical Note 2845. Washington: National Advisory Committee for Aeronautics, December 1952.
5. Hurlbert, F. C. "Electron Beam Density Probe for Measurements in Rarefield Gas Flows." Journal of Applied Physics, 30, No. 3: 273-279 (March 1959).
6. "Instrument Flying." Air Force Manual 51-37. U. S. Government Printing Office, Washington, D. C.: Department of the Air Force, 15 November 1960.
7. Knight, Herbert T., and Douglas Venable. "Apparatus for Precision Flash Radiography of Shock and Detonation Waves in Gases." The Review of Scientific Instruments, 29, No. 2:92-98 (February 1958).
8. Lewis, H. W. "Multiple Scattering in an Infinite Medium." Physical Review, 78:526-529 (June 1950).
9. Price, William J. Nuclear Radiation Detection. New York: McGraw-Hill Book Company, Inc., 1958.
10. "Radioisotopes, Special Materials and Services." Catalog and Price List (3rd Revision). Oak Ridge: Oak Ridge National Laboratory, 1960.
11. "Radiological Health Handbook. Cincinnati: United States Department of Commerce, Office of Technical Services, 1957.
- 11a. Rutherford, Sir Ernest, et al. Radiations from Radioactive Substances. Cambridge: University Press, 1951.

12. Schumacher, B. W. Beta-Ray Gages for Gas Density Measurements. Physic Research Report No. 6001. Toronto: Ontario Research Foundation, 1960.
13. Schumacher, B. W. "Gaging Gas Density with Fast Charged Particles." Nucleonics, 18:109-114 (October 1960).
14. Schumacher, B. W. Improved Density Gage. Record of Invention No. 12. Toronto: Ontario Research Foundation, 1959.
15. Schumacher, B. W. Single-Scattering Density Gage. Record of Invention No. 13. Toronto: Ontario Research Foundation, 5 October 1959.
16. Schumacher, B. W. The Alpha-Particle Thermometer of E. Schopper and D. Knapp. Physics Research Report No. 5804. Toronto: Ontario Research Foundation, 1958.
17. Segre, Emilio, et al. Experimental Nuclear Physics (Vol. I). New York: John Wiley and Sons, Inc., 1953.
- 17a. "Semiconductors, Scintillators, and Pulse Height Analyzers." Nucleonics, 20, No. 5:53 (May 1962).
18. Spencer, L. V. "Theory of Electron Penetration." Physical Review, 98:1597-1615 (June 1955).
19. Tolansky, S., and S. Longman. Introduction to Atomic Physics (Fourth Edition). London: Greene and Co., 1956.
20. Wright, D. E., and D. Hakewessel. Investigation of the Use of Radioisotopes for Extremely High Altitude Measurements. Proposal No. GSDP-218. Durate, California: Giannini Controls Corporation, 1961.

Appendix A

Air and Spacecraft Operating at 100,000 Foot Altitude and Above

Three operational aircraft have approached or exceeded the 100,000 foot altitude. The Navy A3-J Vigilante flown by Commander Leroy A. Heath reached 91,450 feet on December 15, 1960.¹ Another Navy plane, the F4-H Phantom, has zoomed to 98,560 feet.² Captain Joe B. Jorden received the Harmon Trophy for his flight in the F-104-C Starfighter on December 15, 1959, to an altitude of 103,395 feet.

Another Harmon Trophy was awarded in 1961 for the pilot of the experimental rocket aircraft, Major Robert M. White, who established a world altitude record of 217,000 feet which has since been elevated by the same aircraft and pilot to 311,000 feet.³

Colonel Glenn's earth orbital flights on February 20, 1962, in the Mercury capsule were at a minimum altitude of 99 miles (522,720 feet) and a maximum of 162 miles (855,360 feet).⁴ Thus, the altitude capability of five weapons or experimental systems in existence today ranges from 91,000 to 855,000 feet.

¹New York Times, December 16, 1960, page 43, column 2.

²Information from F-110 Systems Project Office, Wright-Patterson Air Force Base, Ohio.

³The Wall Street Journal, July 18, 1962, page 1, column 3.

⁴New York Times, February 20, 1962, page 1.

Looking ahead five years, three new systems are scheduled to be flown at flight altitudes well in excess of 100,000 feet. Gemini will fly, probably in 1963, at about the same altitude as Mercury. Dynasoar, the boost glider, it is believed, can begin short range missions in 1964, and it may be used in elongated elliptical orbits measured in earth radii. For this craft, density altitude information will be critical during the complicated and split-second timed re-entry maneuver beginning at the sensible atmosphere (300,000 feet). Lastly, by 1966, low altitude orbit Apollo shots will begin with the ultimate objective of landing successfully on the moon.

Appendix B

Distinction Between True, Absolute, Pressure, and
Density Altitudes, with Significance of Density
Altitude for Aerodynamic Flight

True altitude means actual height of the aircraft above sea level. Absolute altitude is the height of the local vertical, or the actual height of the aircraft above the surface or terrain over which it is flying. Pressure altitude is the barometric altitude measured above a standard pressure plane, 29.92 inches of mercury. Density altitude is pressure altitude corrected for absolute temperature variations from the standard atmosphere (Ref 6:4-6, 7).

The equations expressing the forces of dynamic pressure, lift, and drag are all direct functions of atmospheric density. While atmospheric density is a function of true altitude, it was shown during the International Geophysical Year that this interrelation varies daily, seasonally, and latitudinally in a complex manner not yet completely known at any one point in space and time. Since these many fluctuations in density may vary by an order of magnitude, and because the aerodynamic equations include density as a parameter, it is seen that any method of altimetry that cannot measure density directly is decidedly limited in usefulness. From a pilot's viewpoint, the situation is this: during a constant mach phase of the mission, the high-altitude winged vehicle is restricted to a flight corridor, above the upper limit of which the vehicle stalls, and below the lower limit of which the skin friction and aerodynamic heating results in structural failure. Both limits are dictated by density, not true, altitude.

Appendix C

Calculation of Theoretical Count Rate as a
Function of Density Altitude Using
Bullard and Massey Graphical Solution

List of Symbols

CR1	= count rate from strontium ⁹⁰ (cps)
CR2	= count rate from yttrium ⁹⁰ (cps)
A	= activity of source (disintegration per second)
μ/ρ	= mass absorption coefficient (cm ² /gm)
ρ_a	= density air (gm/cm ³)
x	= absorption distance (cm)
r_1	= range from source to scatter volume (in.)
N	= number of atmospheric atoms/cm ³
N_0	= Avogadro's Number
I_0	= microscopic scatter cross section (cm ²)
v^e	= energy of electrons in ev
θ	= angle of scatter from path of incidence
Z	= atomic number of target
a_{det}	= area detector (in. ²)
r_2	= range from scatter volume to detector (in. ²)
p	= pressure (mm Hg)
V	= scatter volume

$$CR1 = \frac{A_{Sr} \left\{ e^{-\left(\frac{\mu}{\rho}\right)_{Sr} \rho_a x} \right\}}{4\pi r_1^2} \cdot \frac{N I_{\theta} V a_{det}}{r_2^2} \quad (1)$$

$$CR2 = \frac{A_Y \left\{ e^{-\left(\frac{\mu}{\rho}\right)_Y \rho_a x} \right\}}{4\pi r_1^2} \cdot \frac{N I_{\theta} V a_{det}}{r_2^2} \quad (2)$$

$$A_{Sr} = A_Y = (1/2) (.213) (3.7 \times 10^{10}) \quad (3)$$

1 (footnote)

$$\left(\frac{\mu}{\rho}\right)_{Sr} = \frac{22}{(E_{max})} 1.33 = 42 \quad (4)$$

$$\left(\frac{\mu}{\rho}\right)_Y = 7.8 \quad (5)$$

$$\text{From } p = \rho RT \text{ (perfect gas law)} \quad (6)$$

where $T = 291^{\circ}K$ (from experiment)

$$\rho_a = 1.6p \times 10^{-6} \quad (7)$$

$$x = 200 \text{ cm (from experiment)} \quad (8)$$

$$r_1 = r_2 = 39 \text{ in.} \quad (9)$$

¹Liverhant, S. E. "Elementary Introduction to Nuclear Reactor Physics" New York: John Wiley and Sons, Inc., 1960 (p. 342).

$$N = \frac{\rho N_0}{28.9} = 0.65 \times 10^{17} \text{ p} \quad (10)$$

$$E_{\max} \text{ Y}^{90} = 2.18 \text{ Mev} \quad (11)$$

$$E_{\text{ave}} \text{ Y}^{90} = 0.89 \text{ Mev}^2 \quad (12)$$

$$\sqrt{v'} = 0.94 \times 10^{-3} \text{ ev} \quad (13)$$

$$Z = 7.2 \quad (14)$$

$$\theta = 10 \text{ degrees} \quad (15)$$

$$\frac{\sqrt{v'} \sin 1/2 \theta}{Z^{1/3}} = 42 \text{ Y}^{90} \quad (16)$$

Enter abscissa of Fig. 10 at 42, read ordinate 0.10×10^{-20}

$$I_{\theta \text{ Y}} = (7.2)^{2/3} (0.10 \times 10^{-20}) = .37 \times 10^{-20} \quad (17)$$

In the same way

$$I_{\theta \text{ Sr}} = 2.2 \times 10^{-20} \quad (18)$$

²Hine, G. J. and Gordon L. Brownell. "Radiation Dosimetry." New York: Academic Press, 1956 (p. 698).

From prismoidal formula³

$$V = \frac{h}{6} (A_1 + 4A_2 + A_3) \quad (19)$$

Using as the scattering volume two cylinders, radii 1.1 in. and 0.65 in., intersecting at 10 degrees, it can be shown

$$V \approx 190 \text{ cm}^2 \quad (20)$$

Substituting the now known values into Eqs (1) and (2) and adding gives the final theoretical equation which plots CR as a function of atmospheric pressure.

$$CR = 28pe^{-0.0134p} + 4.5pe^{-.0025p} \quad (21)$$

This equation is plotted in Fig. 10a, page 20; however, pressure has now been changed to the corresponding altitude through use of Appendix D.

The discrepancies between Fig. 10a, the theoretical count rate and Graph IV, the actual count rate, shows that the theory is inadequate to fully explain the actual processes. Considerably more attenuation occurred in the experiment than the theory predicted, and it is suggested this was caused by source energy degradation during source window penetration. Not only would the lower energy betas be more easily absorbed in the lower atmosphere, but since I_0 is strongly energy dependent, the scatter process would also be affected, and these two effects would tend to steepen the slope of the experimental curve during initial climb and to advance the maximum count rate to the right (higher altitudes). The

³Smith, Edward S., et al. "Calculus" New York: John Wiley and Sons, Inc., 1938 (p. 324).

GA/Phys/62-13

too shallow tail of the experimental curve may be explained by the penumbra radiation hypothesis (page 50), although experimental verification of this has not yet been obtained.

Appendix D

Altitude-Pressure Table Used in Environmental Chamber Tests

ALTITUDE PRESSURE TABLE											
ALT.	PRESSURE		ALT.	PRESSURE		ALT.	PRESSURE		ALT.	PRESSURE	
(Feet)	mm.Hg	P.s.i.	(Feet)	mm.Hg	P.s.i.	(Feet)	mm.Hg	P.s.i.	(Feet)	mm.Hg	P.s.i.
0	760.0	14.70	20000	349.1	6.75	40000	140.7	2.72	60000	54.1	1.05
500	746.4	14.43	20500	341.8	6.61	40500	137.4	2.66	60500	52.8	1.02
1000	732.9	14.17	21000	334.6	6.47	41000	134.1	2.59	61000	51.6	0.998
1500	719.7	13.92	21500	327.6	6.33	41500	131.0	2.53	61500	50.4	0.975
2000	706.6	13.66	22000	320.8	6.20	42000	127.9	2.47	62000	49.2	0.951
2500	693.8	13.42	22500	314.0	6.07	42500	124.9	2.42	62500	48.0	0.928
3000	681.1	13.17	23000	307.4	5.94	43000	121.9	2.36	63000	46.9	0.907
3500	668.6	12.93	23500	300.8	5.82	43500	119.0	2.30	63500	45.8	0.886
4000	656.3	12.69	24000	294.4	5.70	44000	116.2	2.25	64000	44.7	0.864
4500	644.2	12.46	24500	288.0	5.57	44500	113.5	2.19	64500	43.6	0.843
5000	632.3	12.23	25000	281.8	5.45	45000	110.9	2.14			
5500	620.6	12.00	25500	275.8	5.33	45500	108.2	2.09			
6000	609.0	11.78	26000	269.8	5.22	46000	105.6	2.04			
6500	597.5	11.55	26500	263.8	5.10	46500	103.1	1.99			
7000	586.4	11.34	27000	258.0	4.99	47000	100.7	1.95	65000	40.6	113.2
7500	575.3	11.12	27500	252.4	4.88	47500	98.3	1.90	66000	36.9	102.9
8000	564.4	10.91	28000	246.8	4.77	48000	96.0	1.86	70000	33.6	93.52
8500	553.7	10.71	28500	241.4	4.67	48500	93.7	1.81	72000	30.4	85.01
9000	543.2	10.50	29000	236.0	4.56	49000	91.5	1.77	74000	27.7	77.26
9500	532.8	10.30	29500	230.6	4.46	49500	89.4	1.73	76000	25.2	70.22
10000	522.6	10.11	30000	225.6	4.36	50000	87.3	1.69	78000	22.9	63.8
10500	512.5	9.91	30500	220.4	4.26	50500	85.2	1.65	80000	20.8	58.01
11000	502.6	9.72	31000	215.4	4.17	51000	83.2	1.61	82000	18.9	52.72
11500	492.8	9.53	31500	210.4	4.07	51500	81.2	1.57	84000	17.2	47.91
12000	483.3	9.35	32000	205.6	3.98	52000	79.3	1.53	86000	15.6	43.55
12500	473.8	9.16	32500	201.0	3.89	52500	77.4	1.50	88000	14.2	39.59
13000	464.5	8.98	33000	196.3	3.80	53000	75.6	1.46	90000	12.9	35.95
13500	455.4	8.81	33500	191.8	3.71	53500	73.8	1.43	92000	11.7	32.7
14000	446.4	8.63	34000	187.3	3.62	54000	72.1	1.39	94000	10.7	29.71
14500	437.5	8.46	34500	183.0	3.54	54500	70.4	1.36	96000	9.7	27.02
15000	428.8	8.29	35000	178.7	3.46	55000	68.8	1.33	98000	8.8	24.55
15500	420.2	8.13	35500	174.4	3.37	55500	67.1	1.30	100000	8.0	22.31
16000	411.8	7.96	36000	170.3	3.29	56000	65.5	1.27	110000	5.0	13.92
16500	403.5	7.80	36500	166.3	3.22	56500	64.0	1.24	120000	3.24	9.026
17000	395.3	7.64	37000	162.4	3.14	57000	62.4	1.21	130000	2.18	6.071
17500	387.3	7.49	37500	158.6	3.07	57500	61.0	1.18	140000	1.51	4.213
18000	379.4	7.34	38000	154.8	2.99	58000	59.5	1.15	150000	1.08	3.003
18500	371.7	7.19	38500	151.2	2.92	58500	58.1	1.12	160000	0.787	2.190
19000	364.0	7.04	39000	147.5	2.85	59000	56.8	1.10	170000	0.583	1.624
19500	356.5	6.89	39500	144.1	2.79	59500	55.4	1.07	180000	0.433	1.206

Appendix E

Altitude-Pressure Table Used in Propulsion Chamber Tests

<u>Altitude</u> <u>Feet</u>	<u>Pressure</u> <u>Microns Hg</u>	<u>Altitude</u> <u>Feet</u>	<u>Pressure</u> <u>Microns Hg</u>
2,000,000	0.0000034	475,000	0.020
1,900,000	0.0000041	450,000	0.030
1,800,000	0.0000057	425,000	0.049
1,700,000	0.0000078	400,000	0.076
1,600,000	0.000011	375,000	0.15
1,500,000	0.000014	350,000	0.25
1,400,000	0.000022	325,000	0.4
1,300,000	0.000031	300,000	1.3
1,200,000	0.000051	290,000	2.2
1,100,000	0.000080	280,000	3.7
1,000,000	0.00014	270,000	6.2
950,000	0.00021	260,000	10
900,000	0.00029	250,000	17
850,000	0.00041	240,000	29
800,000	0.00061	230,000	47
750,000	0.00094	220,000	73
700,000	0.0014	210,000	110
650,000	0.0024	200,000	170
600,000	0.0037	180,000	370
550,000	0.0067	160,000	760
500,000	0.013	140,000	1600

Data from:

1957 alpha, 1957 beta (Sputniks)
 1958 alpha, 1958 gamma (Explorers)

Appendix F

Random Error and Altimeter Lag Error
Analysis of Experimental Small-
Angle-Beta-Scatter-Density Altimeter

Random Error Analysis

The fractional standard deviation for a single instantaneous reading of a count-rate meter is:

$$\frac{\sigma}{Q_m} = \frac{1}{\sqrt{2aRC}} \quad (1)$$

where Q_m = expectation value for the charge at any time, t_0

a = average count rate

RC = time constant

From Graph IV, page 41:

a (cpm)	Altitude (Feet)
24,500	100,000
20,000	110,000
16,000	120,000
12,800	130,000
10,700	140,000
9,200	150,000
8,500	160,000

¹Evans, R. D. "The Atomic Nucleus." New York: 1955 (Page 805).

From Eq (1):

<u>Count Rate Error (cpm)</u>	<u>Altitude Error (feet)</u>
860	1900
780	2000
700	2500
620	3000
580	4000
520	5000
500	7000

The significance of the random error is graphically shown on Graph IVa, page 43.

Altimeter Lag Error Analysis

The maximum vertical velocity, V , of the Titan booster from 100,000 feet to 200,000 feet is 1700 feet per second,² and time constant, T , of the experimental beta-scatter altimeter count rate meter is 1 second. The combination of a rapid climb rate and a time constant of 1 second produces an altimeter lag, and it is the purpose of this appendix to determine the amount of that lag.

In an RC network, let q = charge, C = capacitance, v = voltage, and R = resistance. Then

$$\frac{dq}{dt} = C \frac{dv}{dt} + \frac{v}{R} \quad (2)$$

In a count rate meter let a = average count rate and b = the constant pulse height necessary to give one count. Then

²Belcher, Paul. Personal Communication. ASNRFA, Wright-Patterson Air Force Base, Ohio. (July 1962).

$$a\delta = \frac{dq}{dt} \quad (3)$$

Equating Eqs (2) and (3) we have

$$\frac{a\delta}{C} = \frac{dv}{dt} + \frac{v}{RC} \quad (4)$$

The solution of which is

$$a = \frac{v}{R\delta (1 - e^{-t/RC})} \quad (5)$$

Assuming that the change in count rate with change in altitude, h , is a decreasing exponential function, the count rate may be written as a function of time where k is a constant.

$$a(t) = a'e^{-k(Vt + h_0)} \quad (6)$$

Making use of the steady state value of $a' = \frac{v'}{R\delta}$ and substituting the boundary condition that $t = 0$, $v = v'$, Eq (2) can be solved through use of the integrating factor $e^{t/RC}$ to obtain the following:

$$\frac{v(t)}{v'} = \frac{1}{1 - kV} \left\{ e^{-kVt} - e^{-t/T} \right\} + e^{-t/T} \quad (7)$$

Equation (7), when inserted into a computer by the program shown below with $V = 1700$ ft/sec and $T = 1$ sec., showed an altimeter lag error of 1100 feet in the 100,000 foot to 160,000 foot range. This result is graphically depicted in Graph IVa, page 43.

The combination of the two errors of altitude lag and random statistical fluctuations suggests an optimization is possible. Through an iterative computer program, $T = 2$ sec. was found to minimize the

GA/Phys/62-13

total error for the Titan boost mission (least error was 8000 feet at 160,000 feet). For minimization of total error, large T should be used for low vertical velocity missions, small T for high vertical velocity missions.

```
08000      DIMENSION Q(15)
08000 1     ACCEPT,TAU,CK
08036      T=0.
08060      I = 1
08084      A=1./(1.-CK*TAU)
08156 5     F=EXP(-T/TAU)
08216      Q(I) = A*(EXP(-CK*T)-F) + F
08336      PRINT 9, T, Q(I)
08396      I=I+1
08432      T=T+5.
08468      IF(11-I) 7,5,5
08536 7     GO TO 1
08544 9     FORMAT(/F5.1,F9.3)
08576      END
END OF COMPILATION 09241T9530
```

Vita

Alexander K. Rupp was born on [REDACTED], the son of Dr. Charles A. Rupp and Luella K. Rupp. He graduated from Central High School in Washington, D. C. on 30 May 1948, entered the United States Military Academy on 5 July 1951, and received his diploma and Air Force Commission on 3 June 1955. After receiving his pilot rating on 14 August 1956, he spent four years as a fighter pilot stationed in Germany where he married Ruth Michels, who is the mother of their two children, Alexander and Karen Monica. From 18 August 1960 to 10 August 1962, he studied astronautics at the Air Force Institute of Technology, and on 26 August 1962 he reported to Edwards Air Force Base, California, to enter the Experimental Test Pilot School.

Permanent address: [REDACTED]

This thesis was typed by Mrs. Marian M. Whitaker.

UNCLASSIFIED

UNCLASSIFIED